Techniques and Unique and Characteristic Signatures to Identify Hydrino are Predicted from Exact Closed-Form Solutions of Atoms and Molecules

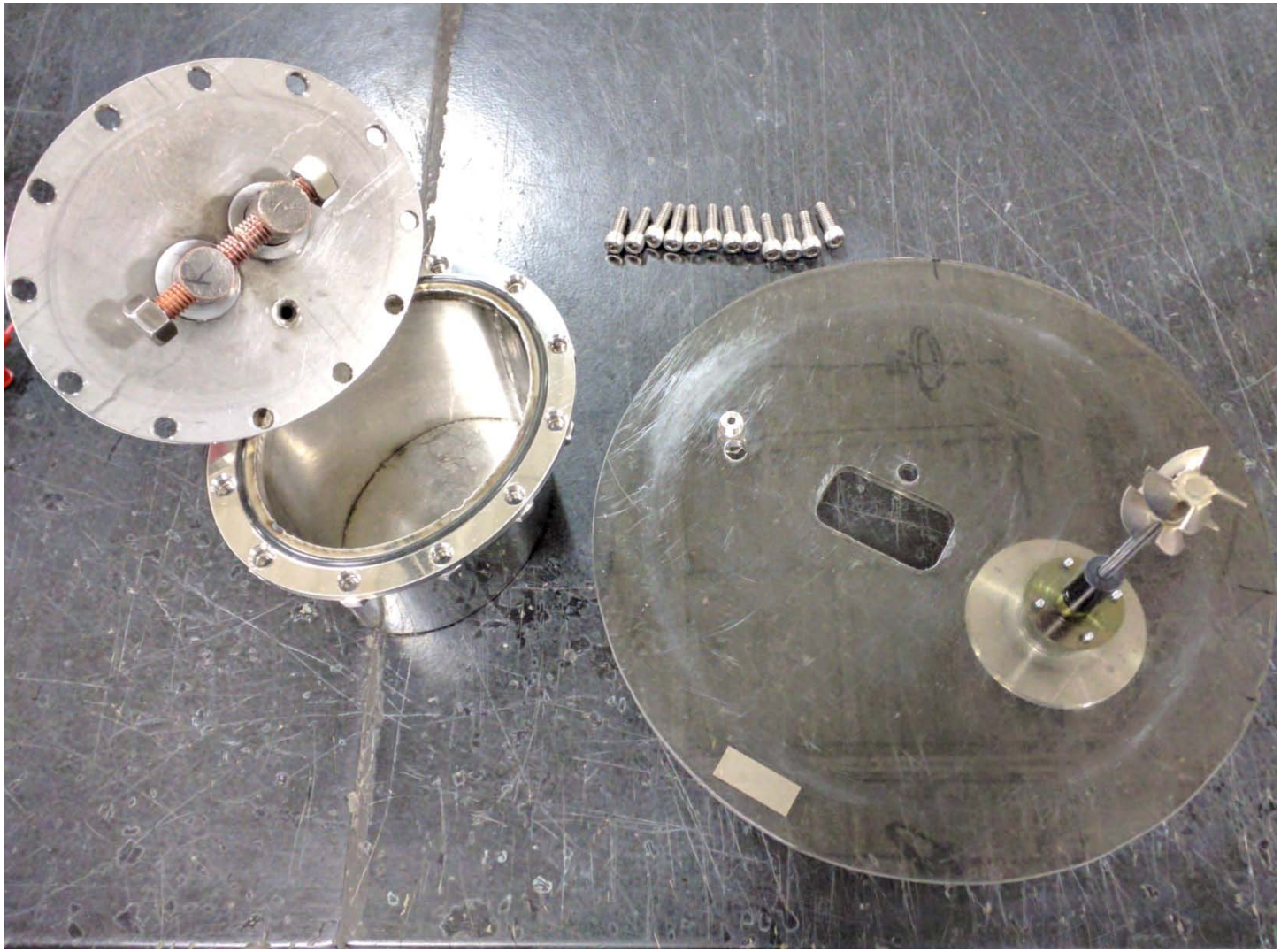

Bomb Calorimetry on Hydrated Silver Shot Detonation

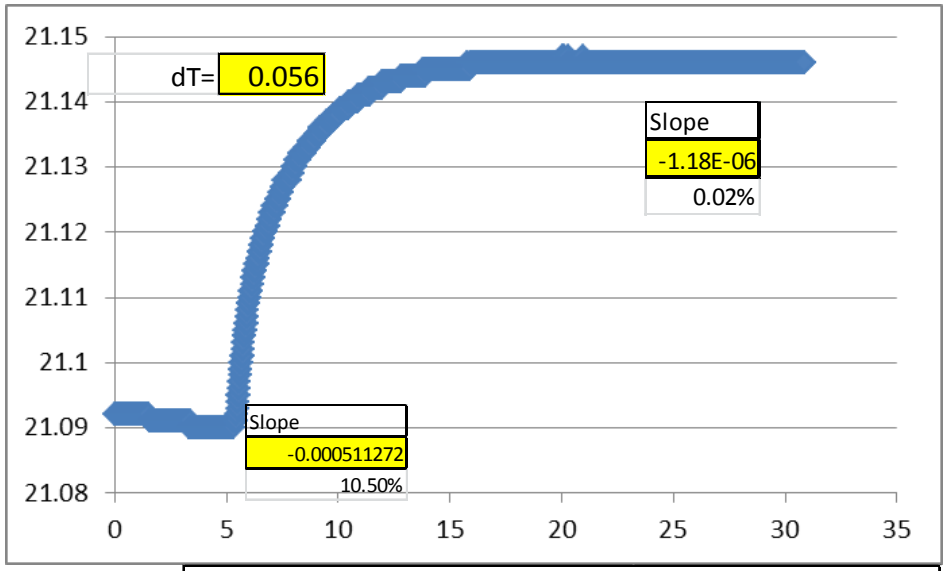

Parr Analysis	
Total Temp Rise (oC)	0.056
60% Temp Rise	0.0336
Temp of 60% T Rise, tb	21.1236
Time of 60% T Rise, b	7.016666667
Firing Temp, Ta	21.09
Firing Time, a	5.116666667
Heat End Temp, Tc	21.146
Heat End Time, c	16.58333333
r1	-0.000511272
r2	-1.17582E-06
dT=Tc - Ta - r1*(b-a)-r2*(c-b)	0.056982665
Cp	12300
Eout =Cp*dT (J)	700.89
Ein (J)	189.00
dE (J)	511.89
Excess (X)	3.71

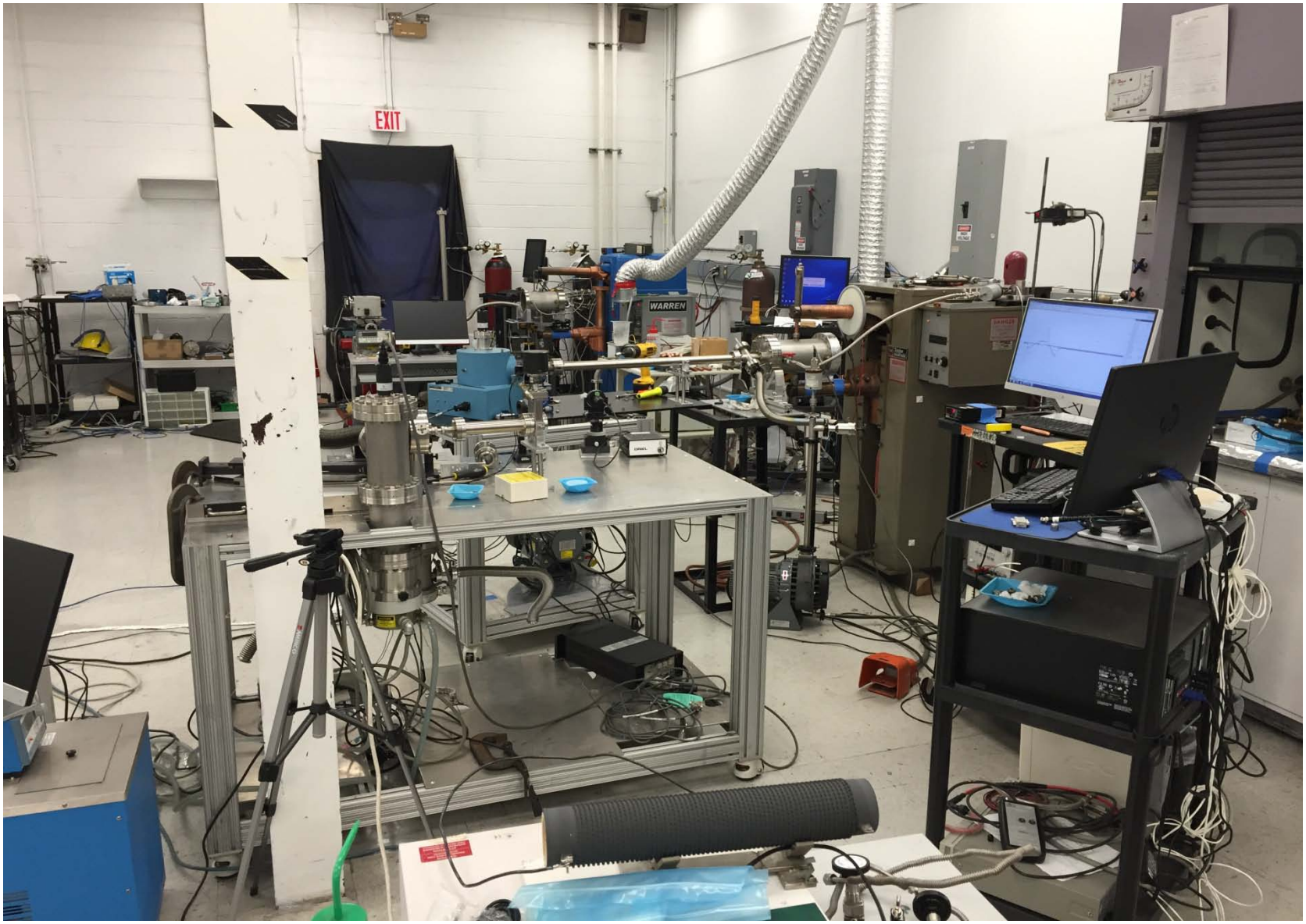
EXIT
WARREN

Hydrino Reaction ("BlackLight Process")

1. Atomic hydrogen reacts with an energy acceptor called a catalyst wherein energy is transferred from atomic hydrogen to the catalyst which forms an ion due to accepting the energy
2. Then, the negative electron drops to a lower shell closer to the positive proton to form a smaller hydrogen atom called a "hydrino" releasing energy that ultimately is in the form of heat
3. The catalyst ion regains its lost electrons to reform the catalyst for another cycle with the release of the initial energy accepted from hydrogen. With the imposition of an arc current condition, the limiting space charge of the ionized electrons is eliminated and the rate becomes massively high.

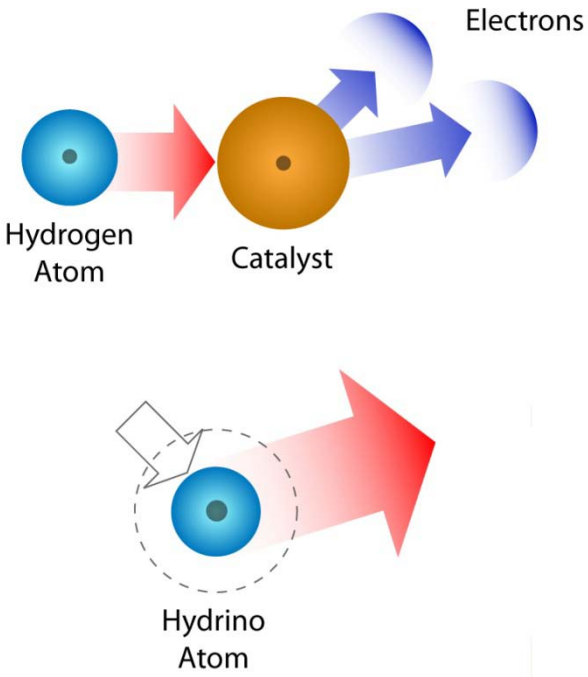

Optical Power Measurement Using NIST Standard Over the UV Region: Spectral Emission in the High Energy Region Only

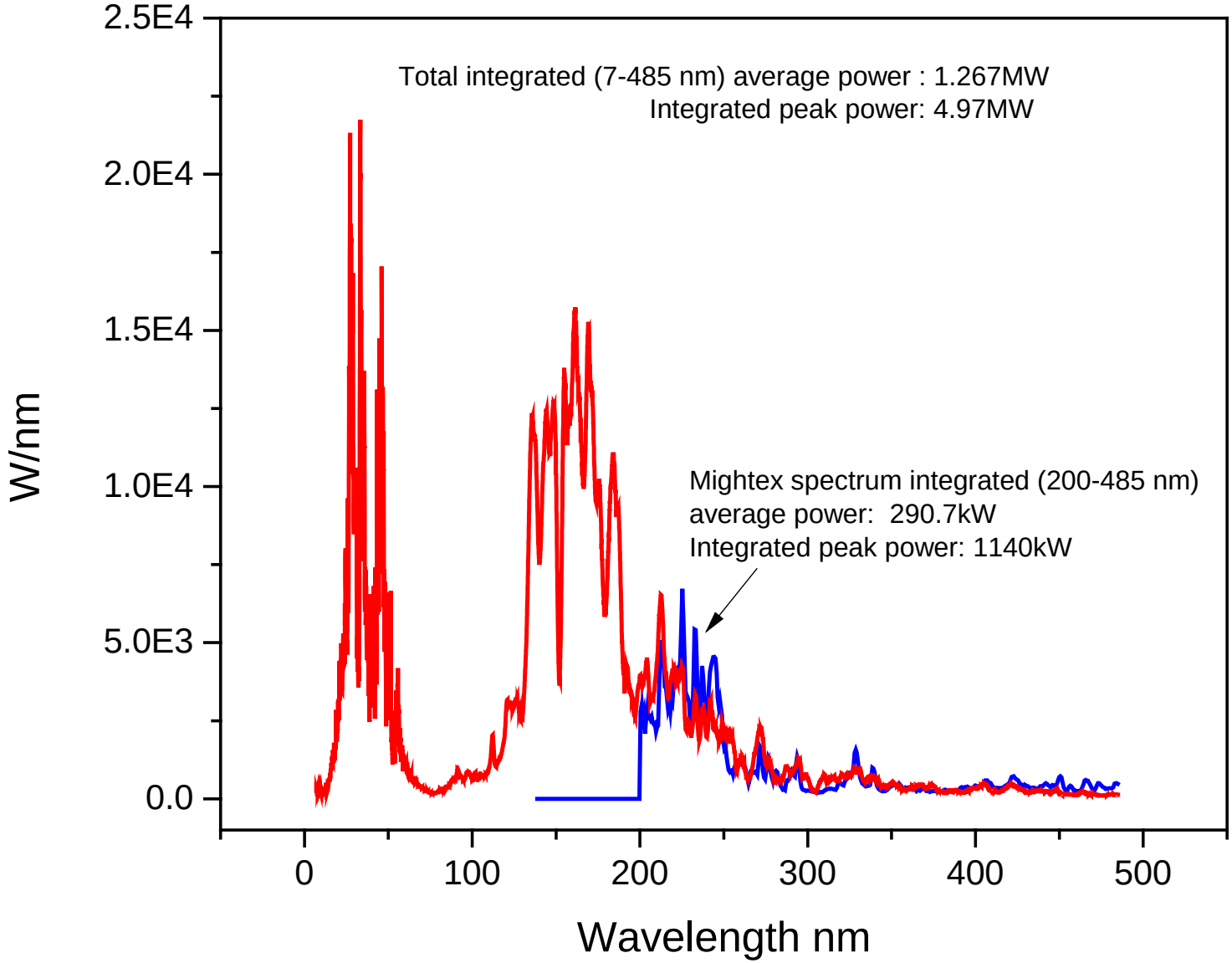

Novel Hydrino Compounds

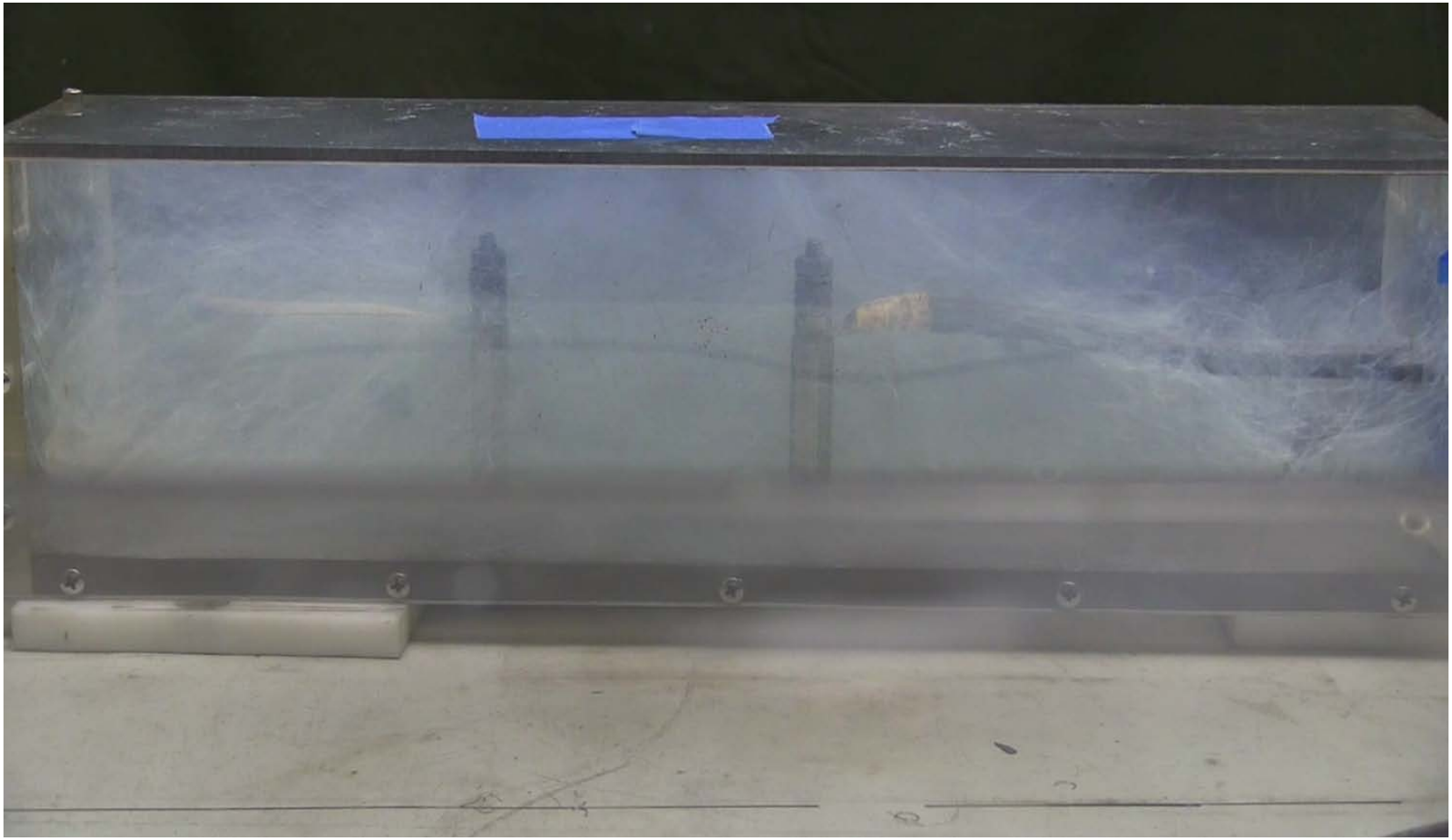

Novel Hydrino Compounds

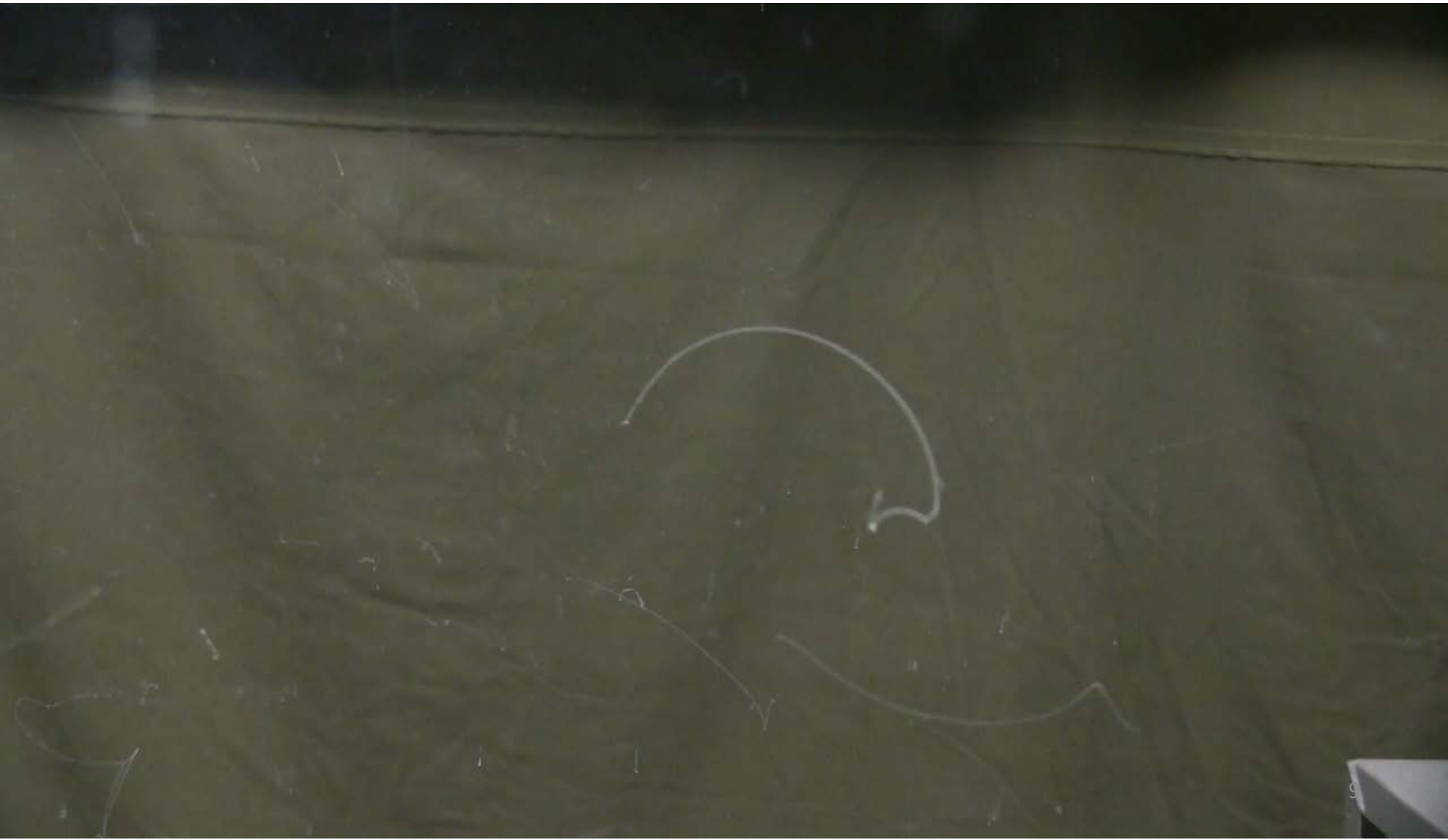

Novel Hydrino Compounds

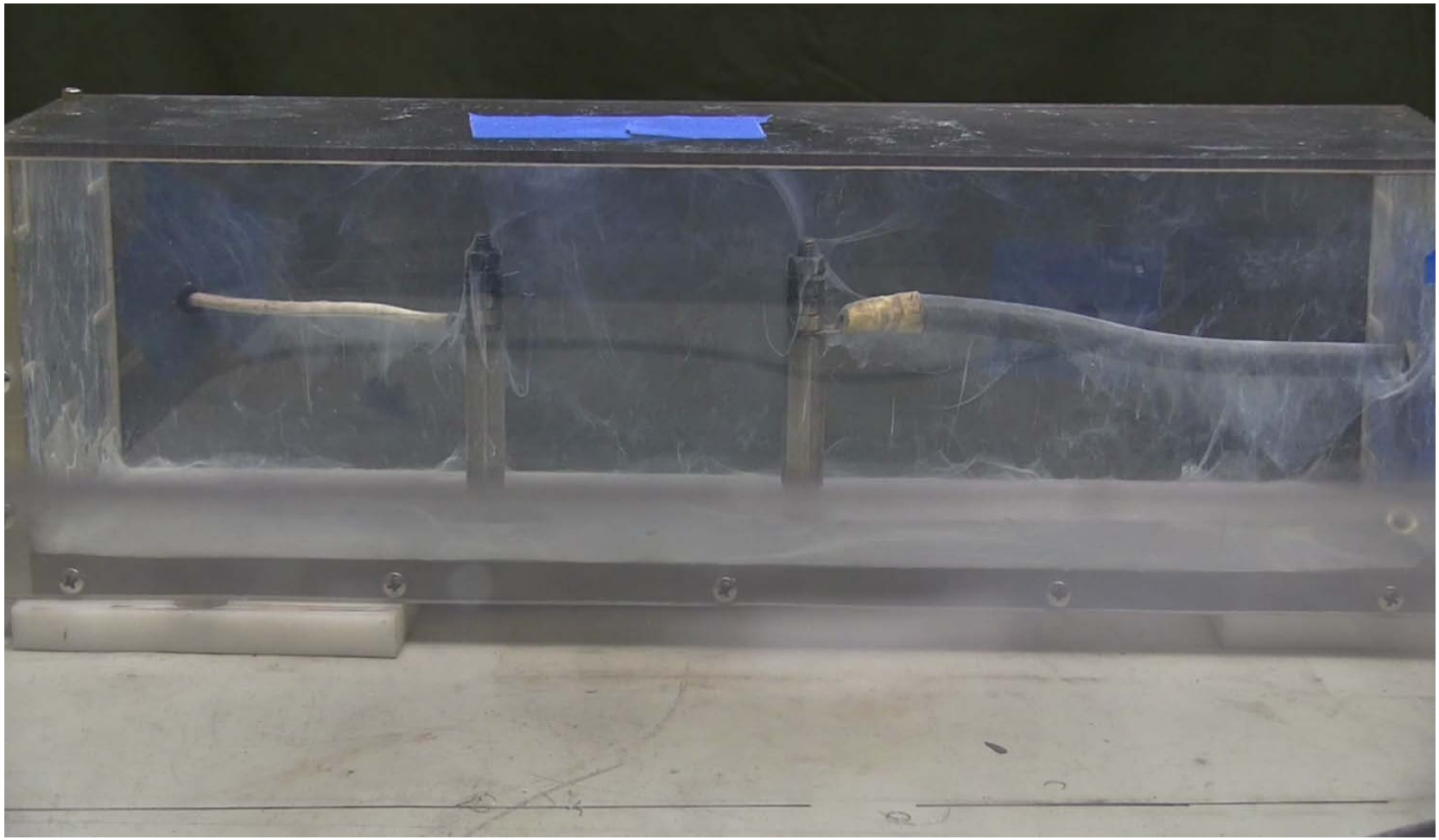

Novel Hydrino Compounds

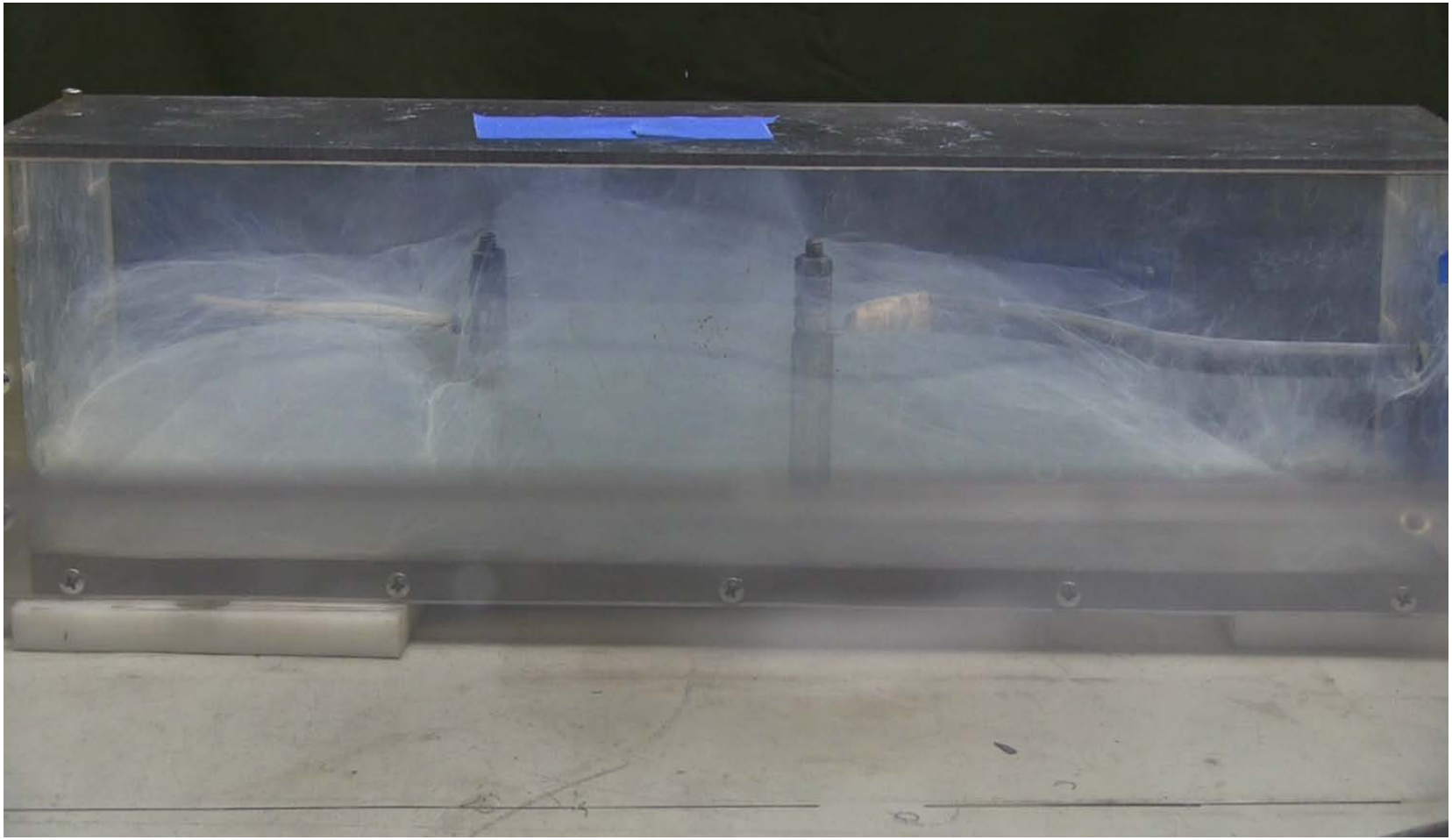

Novel Hydrino Compounds

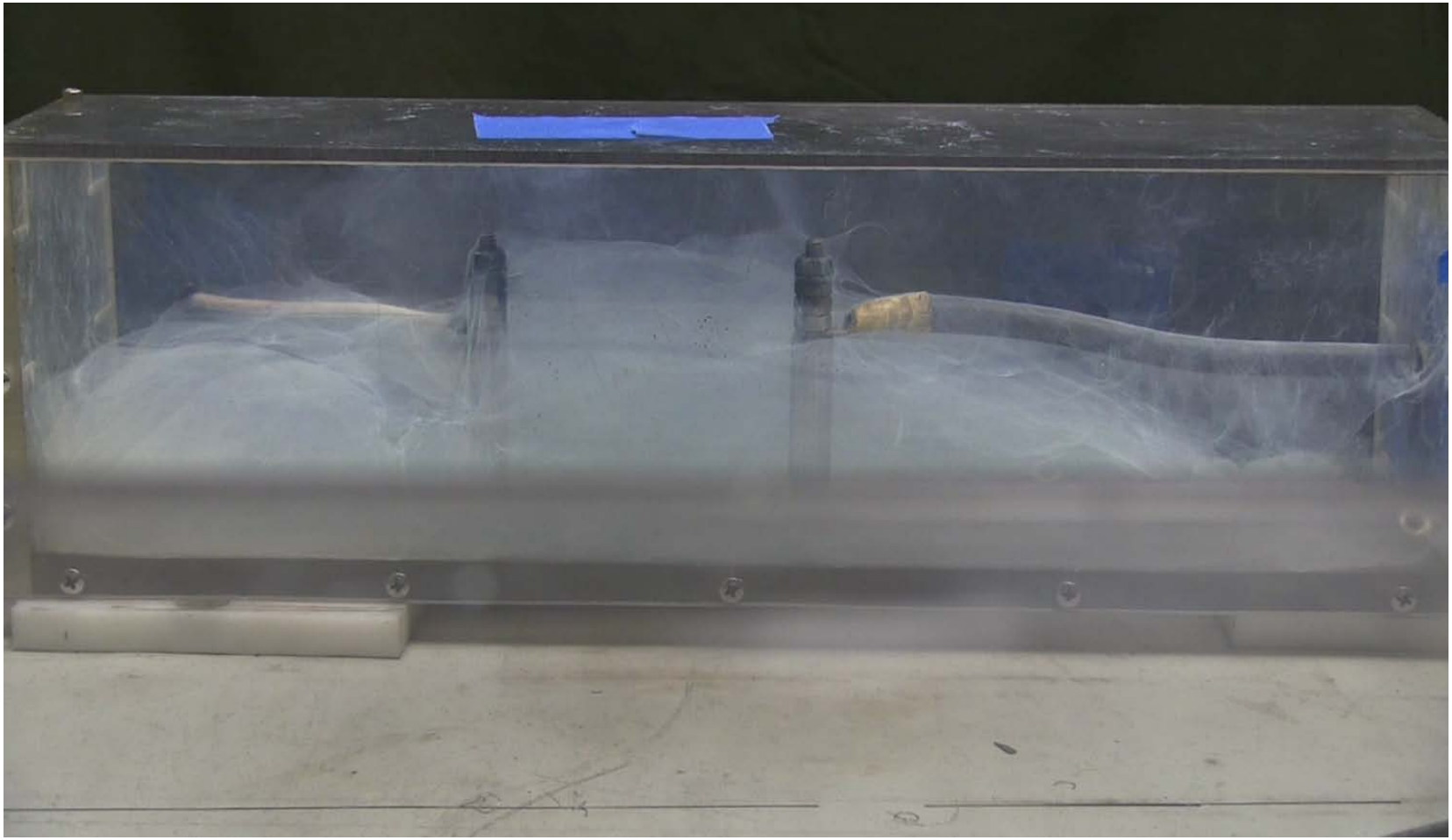

Novel Hydrino Compounds

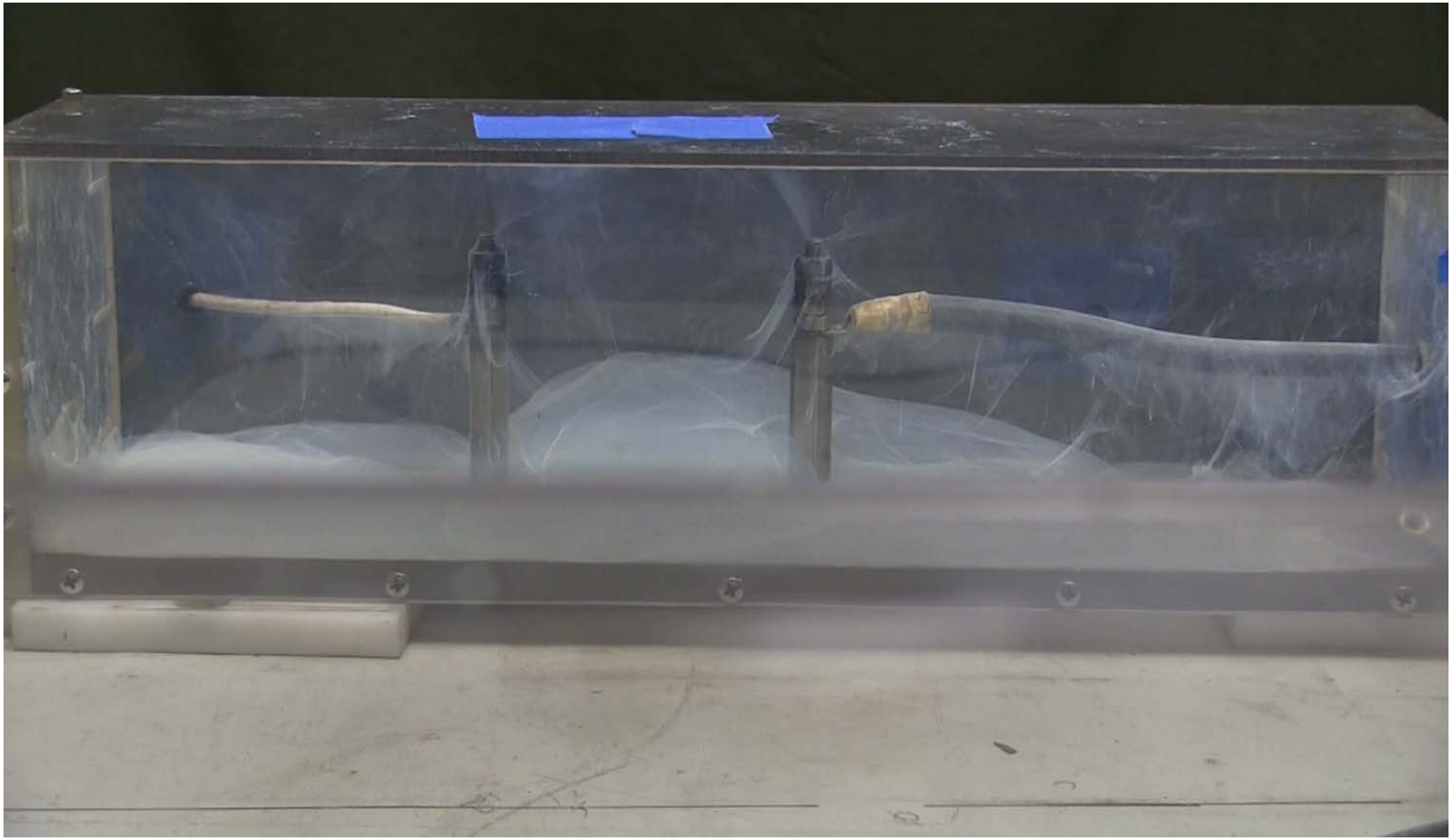

Novel Hydrino Compounds

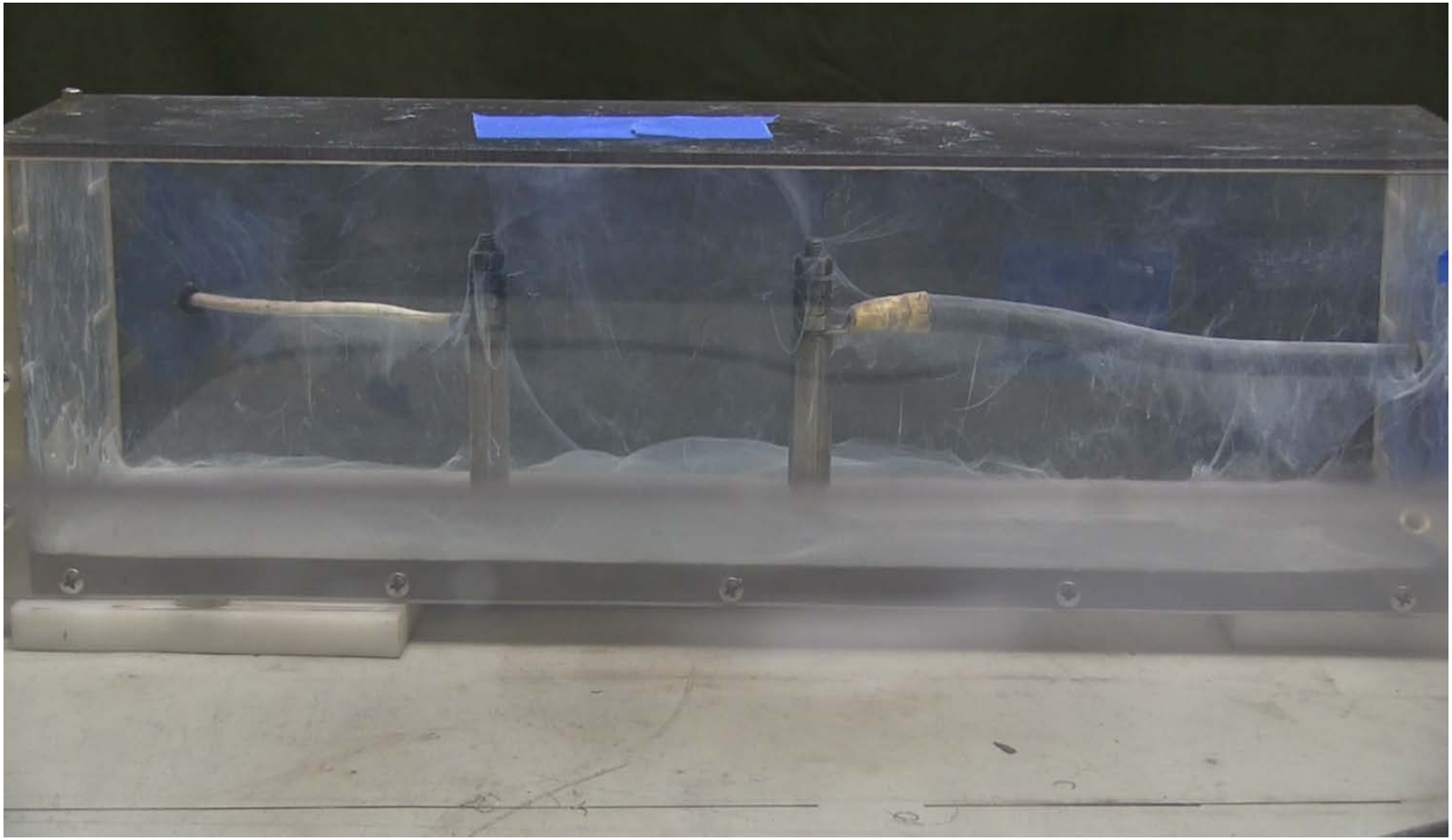

Methods for measuring Hydrino® product

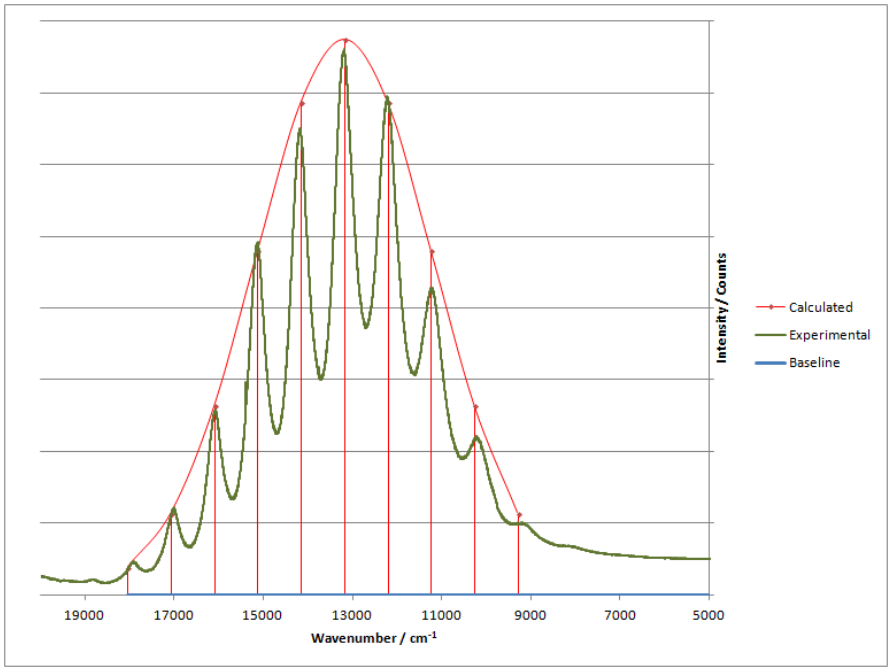

- GUT
- Molecular modeling
- H(1/2) and H(1/4) hydrino transitions observed by continuum radiation
- Astronomy data verifying hydrinos such as H(1/2), H(1/3), and H(1/4) hydrino transitions
- H (1/4) spin-nuclear hyperfine transition
- Hydrino trapped on witness plates and in alkali halide-hydride crystals
- Polymeric molecular hydrino compounds
- In situ H_2 (1/4) gas synthesis in argon and analysis

- H_2 (1/4) ro-vib spectrum in crystals by e-beam excitation emission spectroscopy
- H_2 (1/4) X-ray photoelectron spectroscopy (XPS) binding energy
- H_2 (1/4) Fourier Transform Infrared (FTIR)
- H_2 (1/4) Inverse Raman effect (IRE)
- H_2 (1/4) Photoluminescence spectroscopy
- Electron Paramagnetic Resonance Spectroscopy (EPR)
- Time of Flight Secondary Ion Mass Spectroscopy (ToF-SIMs) and Electrospray Ionization Time of Flight (ESI-ToF) identification of hydrino compounds
- MAS H NMR
- Thermogravimetric analysis (TGA)
- Cryogenic gas chromatography
- Fast H in plasma including microwave and rt-plasmas
- Rt-plasma with filament and discharge
- Afterglow
- Highly pumped states
- H inversion
- Commercial differential scanning calorimetric (DSC) and water flow calorimetry with multiple solid fuels chemistries
- Arbin-Instrument measured electricity gain over theoretical in CIHT cells
- SunCell® fully ionized energetic plasma and electromagnetic pulse
- 20 MW extreme ultraviolet NIST-calibrated optically measured power in shot blasts
- Commercial bomb calorimetry of energetic shots
- Shock wave 10X TNT

Identification of Molecular Hydrino

by the Gold Standard:
Rotational Energies
that Match the Predicted p^2 energies of H_2

Exact Closed-Form Solutions of H_2^+ and H_2

The Laplacian in ellipsoidal coordinates is solved with the constraint of nonradiation

$$(\eta-\zeta)R_\xi\frac{\partial}{\partial\xi}(R_\xi\frac{\partial\varphi}{\partial\xi})+(\zeta-\xi)R_\eta\frac{\partial}{\partial\eta}(R_\eta\frac{\partial\varphi}{\partial\eta})+(\xi-\eta)R_\zeta\frac{\partial}{\partial\zeta}(R_\zeta\frac{\partial\varphi}{\partial\zeta})=0$$

The total energy of the hydrogen molecular ion having a central field of $+pe$ **at each focus of the prolate spheroid molecular orbital**

$$E_T=-p^2\left\{\frac{e^2}{8\pi\varepsilon_o a_{\mathrm{H}}}(4\ln 3-1-2\ln 3)\left[1+\sqrt{\frac{2\hbar\sqrt{\dfrac{2e^2}{4\pi\varepsilon_o\left(2a_{\mathrm{H}}\right)^3}}}{m_e}}{m_e c^2}\right]-\frac{1}{2}\hbar\sqrt{\frac{k}{\mu}}\right\}=-p^2 16.13392\ eV-p^3 0.118755\ eV$$

The total energy of the hydrogen molecule having a central field of $+pe$ **at each focus of the prolate spheroid molecular orbital**

$$E_T=-p^2\left\{\frac{e^2}{8\pi\varepsilon_o a_0}\left[\left(2\sqrt{2}-\sqrt{2}+\frac{\sqrt{2}}{2}\right)\ln\frac{\sqrt{2}+1}{\sqrt{2}-1}-\sqrt{2}\right]\left[1+p\sqrt{\frac{2\hbar\sqrt{\dfrac{e^2}{4\pi\varepsilon_o a_0^3}}}{m_e}}{m_e c^2}\right]-\frac{1}{2}\hbar\sqrt{\frac{k}{\mu}}\right\}=-p^2 31.351\ eV-p^3 0.326469\ eV$$

The Nature of the Chemical Bond of Hydrogen cont'd

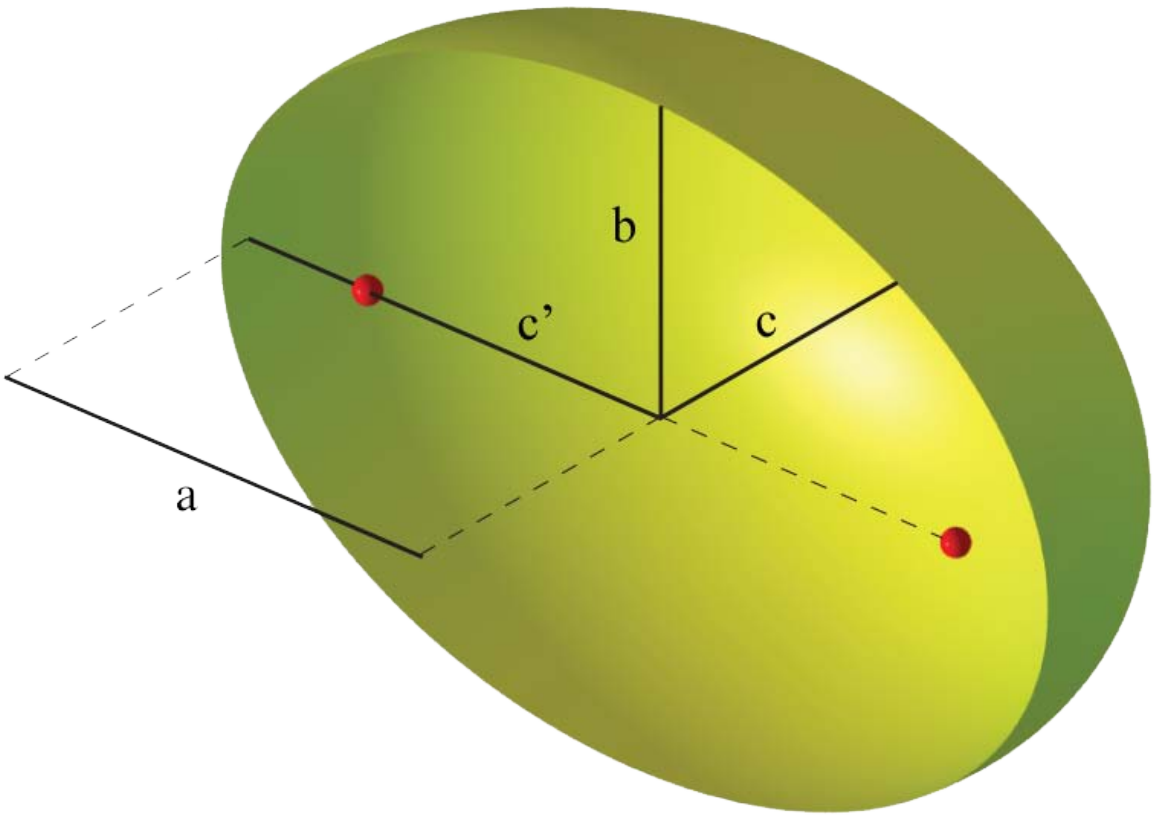

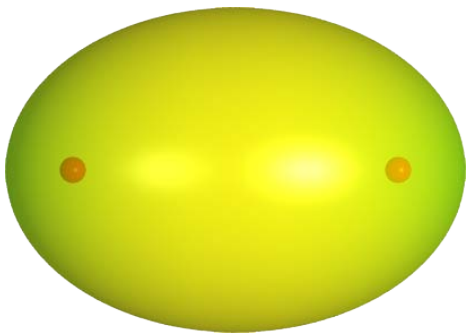

Front view

The Internuclear Distance, $2c'$, which is the distance between the foci is $2c' = \sqrt{2}a_o$.

The experimental internuclear distance is $\sqrt{2}a_o$.

The Semiminor Axis, b, is $b = \frac{1}{\sqrt{2}}a_o$ The Eccentricity, e, is $e = \frac{1}{\sqrt{2}}$

Charge-Density Function

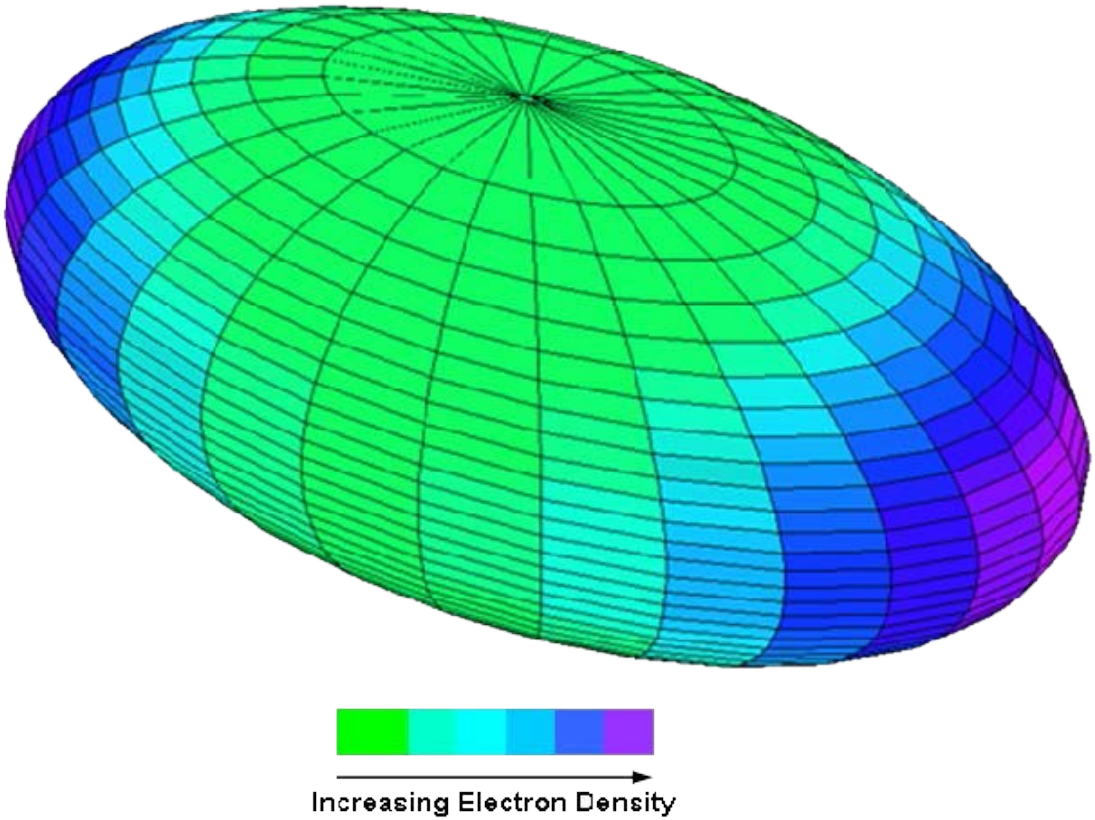

Click the above image to view animation online

Molecular Orbital Current Corresponding to Electron Spin s=1/2

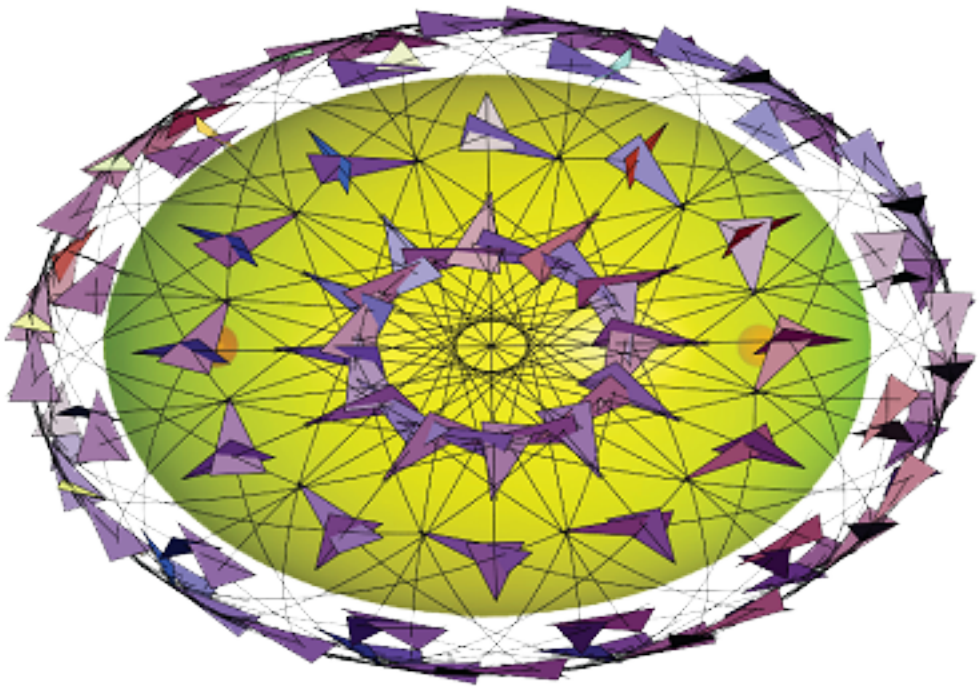

A representation of the z-axis view of the continuous charge-density and supercurrent-density distributions of the MO with 144 vectors overlaid giving the direction of the currents (nuclei not to scale).

The calculated and experimental parameters of H_2, D_2, H_2^+ and D_2^+.

Parameter	Calculated	Experimental	Eqs.	Ref. for Exp.
H_2 Bond Energy	4.478 eV	4.478 eV	11.300	24
D_2 Bond Energy	4.556 eV	4.556 eV	11.302	24
H_2^+ Bond Energy	2.654 eV	2.651 eV	11.269	24
D_2^+ Bond Energy	2.696 eV	2.691 eV	11.271	25
H_2 Total Energy	31.677 eV	31.675 eV	11.296	24, 30, 19[a]
D_2 Total Energy	31.760 eV	31.760 eV	11.297	20, 25[b]
H_2 Ionization Energy	15.425 eV	15.426 eV	11.298	30
D_2 Ionization Energy	15.463 eV	15.466 eV	11.299	25
H_2^+ Ionization Energy	16.253 eV	16.250 eV	11.267	24, 19[c]
D_2^+ Ionization Energy	16.299 eV	16.294 eV	11.268	20, 25[d]
H_2^+ Spin Magnetic Moment	$\frac{\mu_B}{2}$	$\frac{\mu_B}{2}$	12.24	31
Absolute H_2 Gas-Phase NMR Shift	-28.0 ppm	-28.0 ppm	11.416	32-33
H_2 Quadrupole Moment	0.4764×10^{-16} cm^2	$0.38 \pm 0.15 \times 10^{-16}$ cm^2	11.430-11.431	46
H_2 Internuclear Distance[e]	0.748 Å $\sqrt{2}a_o$	0.741 Å	11.287	34
D_2 Internuclear Distance[e]	0.748 Å $\sqrt{2}a_o$	0.741 Å	11.287	34
H_2^+ Internuclear Distance[f]	1.058 Å $2a_o$	1.06 Å	11.256	24
D_2^+ Internuclear Distance[e]	1.058 Å $2a_o$	1.0559 Å	11.256	25
H_2 Vibrational Energy	0.517 eV	0.516 eV	11.308	27, 28
D_2 Vibrational Energy	0.371 eV	0.371 eV	11.313	14, 20
H_2 $\omega_e x_e$	120.4 cm^{-1}	121.33 cm^{-1}	11.310	25
D_2 $\omega_e x_e$	60.93 cm^{-1}	61.82 cm^{-1}	11.314	20
H_2^+ Vibrational Energy	0.270 eV	0.271 eV	11.277	14, 20
D_2^+ Vibrational Energy	0.193 eV	0.196 eV	11.281	20
H_2 J=1 to J=0 Rotational Energy[e]	0.0148 eV	0.01509 eV	12.74	24
D_2 J=1 to J=0 Rotational Energy[e]	0.00741 eV	0.00755 eV	12.66-12.74	24
H_2^+ J=1 to J=0 Rotational Energy[f]	0.00740 eV	0.00739 eV	12.78	24
D_2^+ J=1 to J=0 Rotational Energy[e]	0.00370 eV	0.003723 eV	12.66-12.71, 12.78	25

[a] The experimental total energy of the hydrogen molecule is given by adding the first (15.42593 *eV*) [30] and second (16.2494 *eV*) ionization energies where the second ionization energy is given by the addition of the ionization energy of the hydrogen atom (13.59844 *eV*) [19] and the bond energy of H_2^+ (2.651 *eV*) [24].

[b] The experimental total energy of the deuterium molecule is given by adding the first (15.466 *eV*) [25] and second (16.294 *eV*) ionization energies where the second ionization energy is given by the addition of the ionization energy of the deuterium atom (13.603 *eV*) [20] and the bond energy of D_2^+ (2.692 *eV*) [25].

[c] The experimental second ionization energy of the hydrogen molecule, IP_2, is given by the sum of the ionization energy of the hydrogen atom (13.59844 *eV*) [19] and the bond energy of H_2^+ (2.651 *eV*) [24].

[d] The experimental second ionization energy of the deuterium molecule, IP_2, is given by the sum of the ionization energy of the deuterium atom (13.603 *eV*) [20] and the bond energy of D_2^+ (2.692 *eV*) [25].

[e] The internuclear distances are not corrected for the reduction due to $\overline{E}_{osc}$.

[f] The internuclear distances are not corrected for the increase due to $\overline{E}_{acc}$.

HOH-Argon E-beam Emission
Hydrino $H_2(1/4)$ Ro-vibrational P Branch

N101403/2004

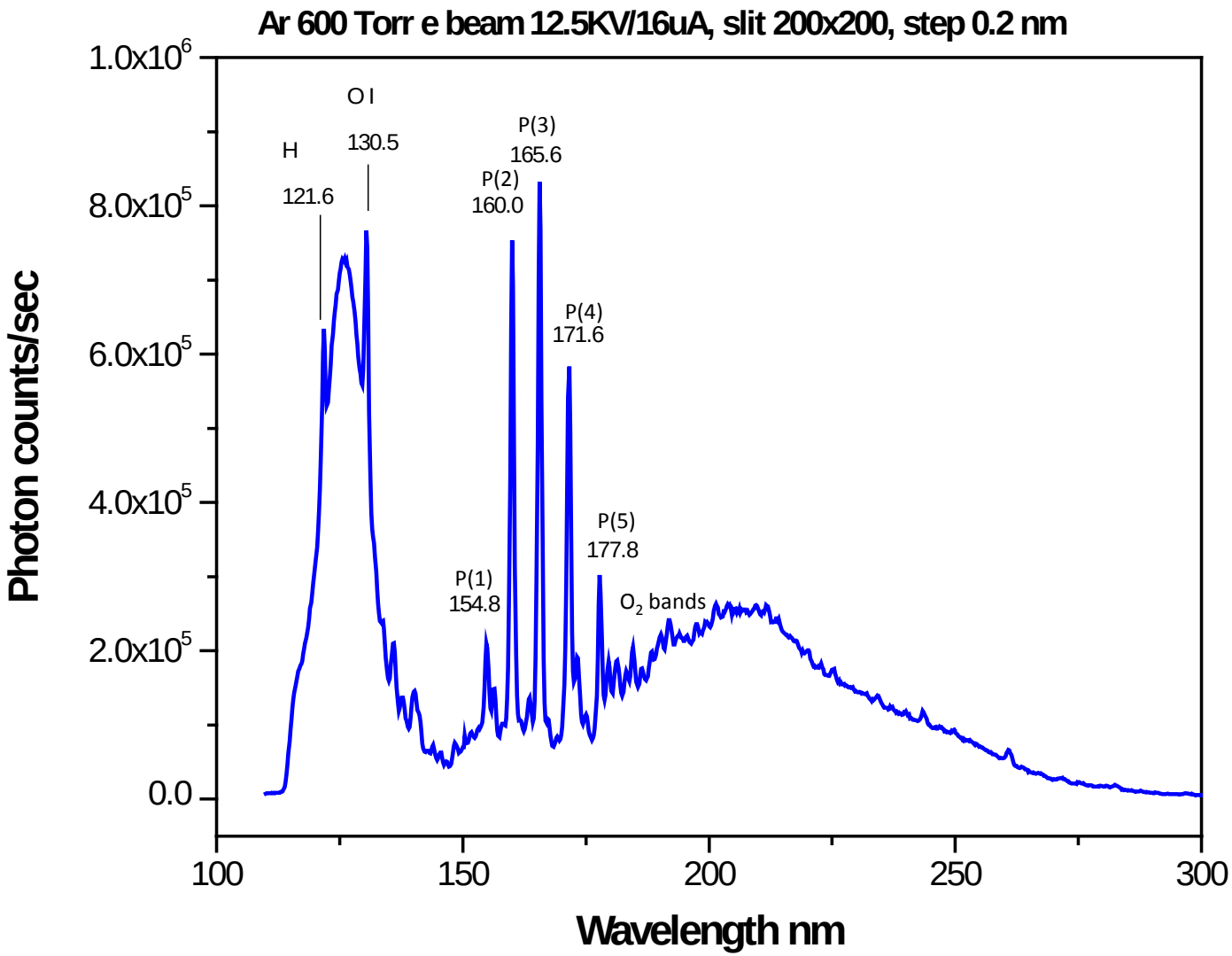

HOH-Argon E-beam Emission
Hydrino $H_2(1/4)$ Ro-vibrational P Branch

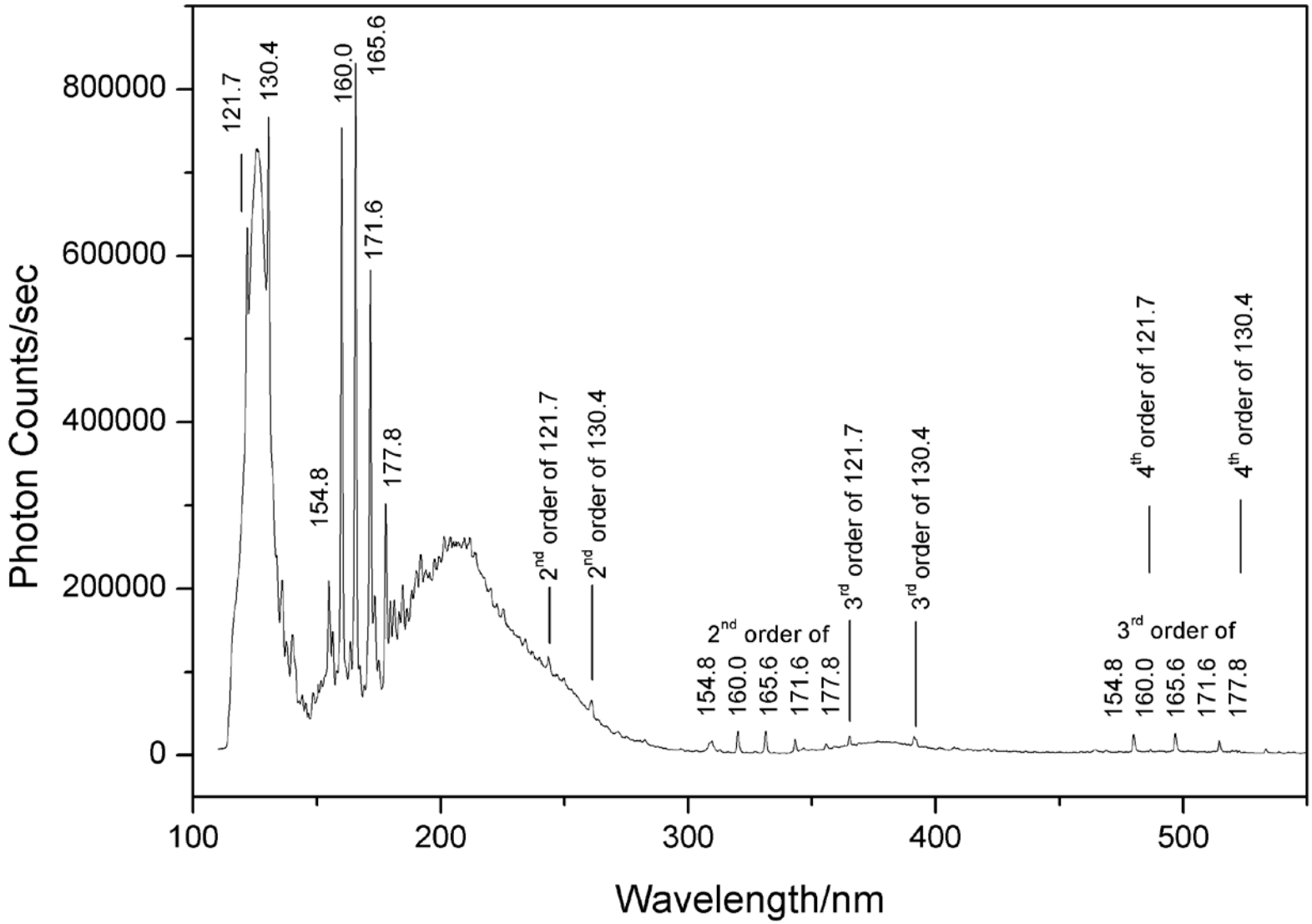

HOH Catalyst Confirmation by Relationship of the Corresponding OH-band Intensity to the Molecular Hydrino $H_2(1/4)$ Ro-vibrational Band

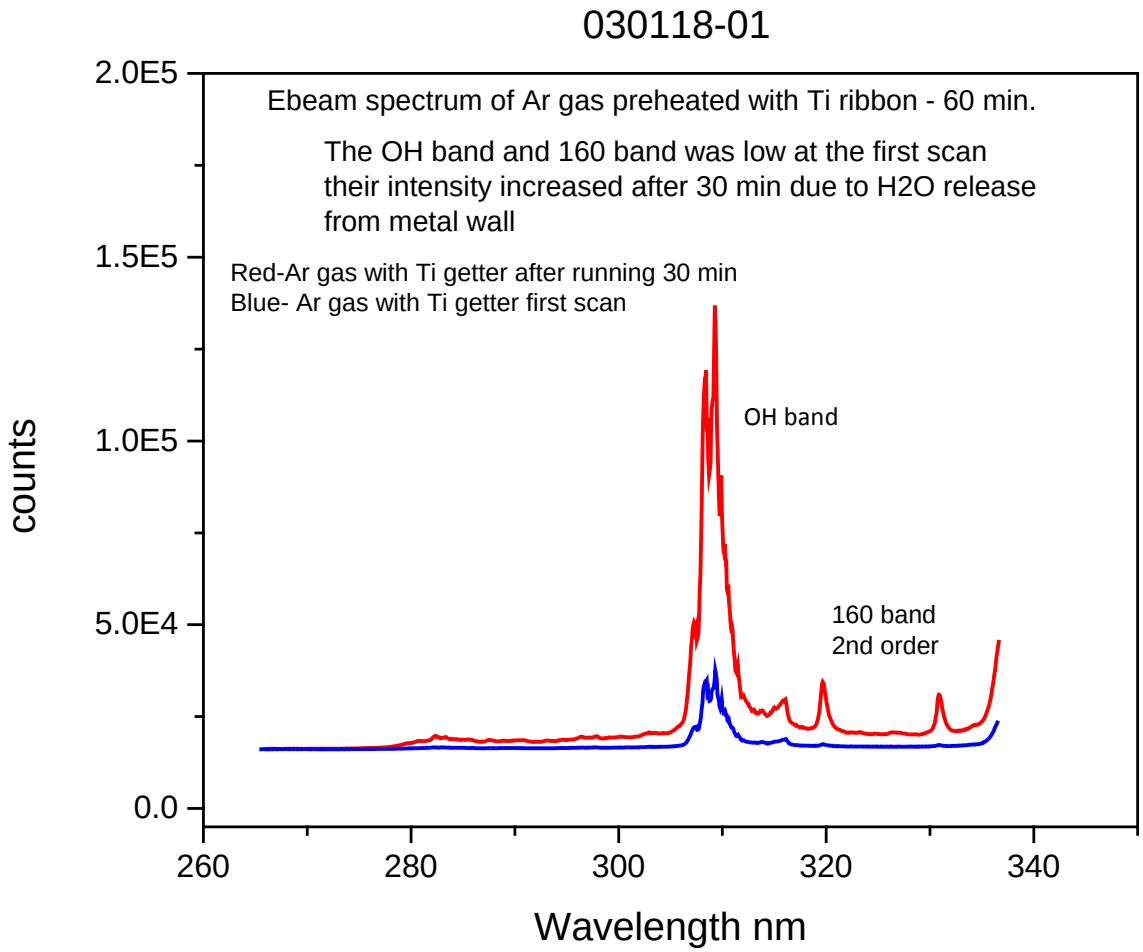

HOH Catalyst Confirmation by Relationship of the Corresponding OH-band Intensity to the Molecular Hydrino $H_2(1/4)$ Ro-vibrational Band

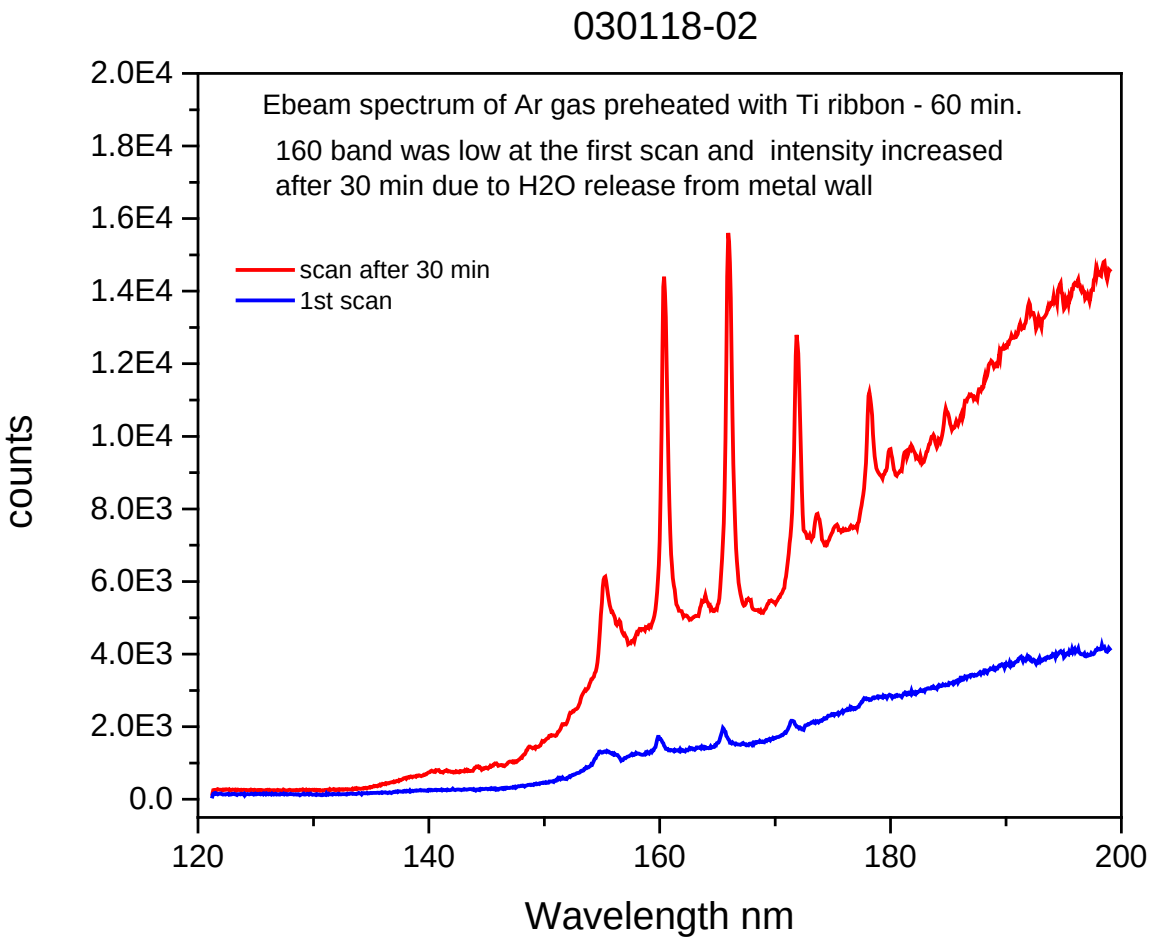

HOH Catalyst Confirmation by Relationship of the HOH Addition to the Molecular Hydrino $H_2(1/4)$ Ro-vibrational Band (Ti getter processed dry argon)

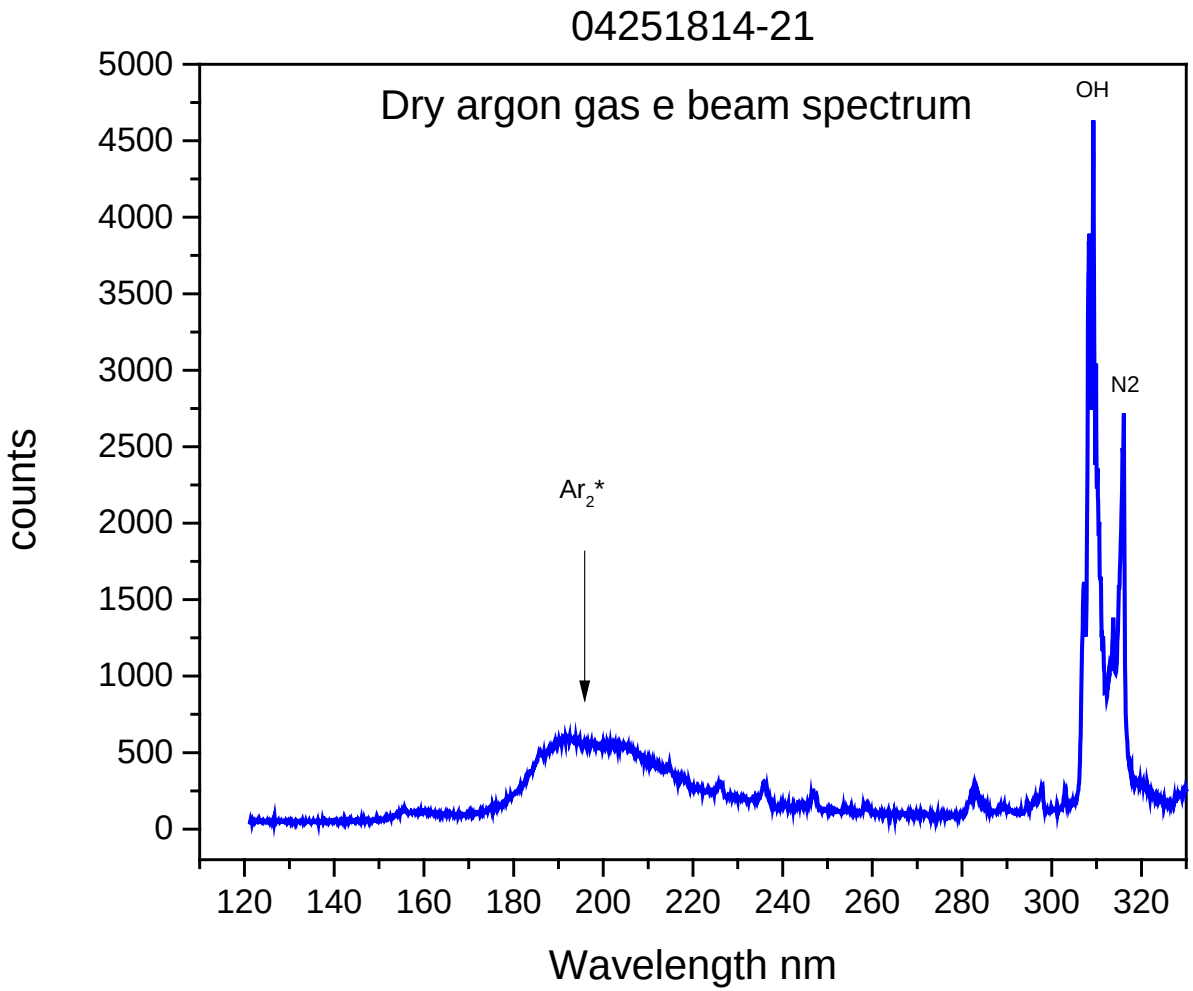

HOH Catalyst Confirmation by Relationship of the HOH Addition to the Molecular Hydrino $H_2(1/4)$ Ro-vibrational Band (argon containing water vapor 10X increase of OH band)

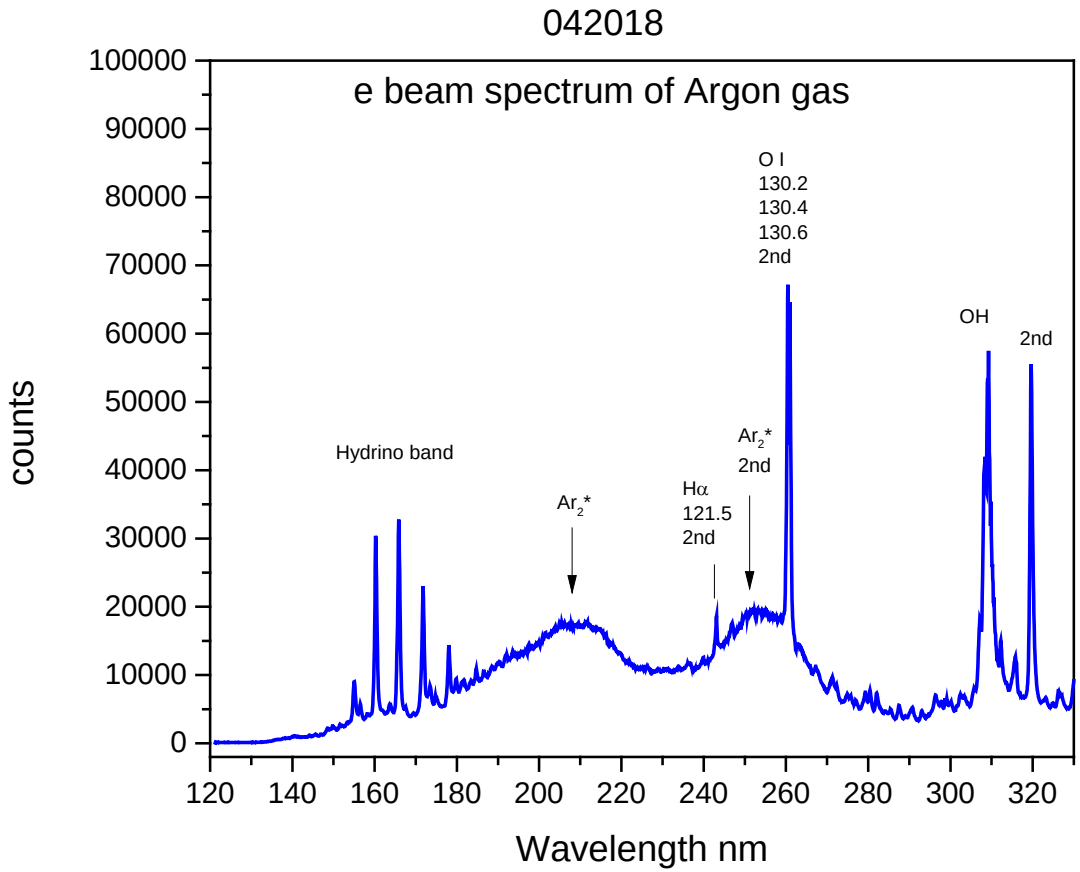

HOH-Argon E-beam Emission Linear Regression

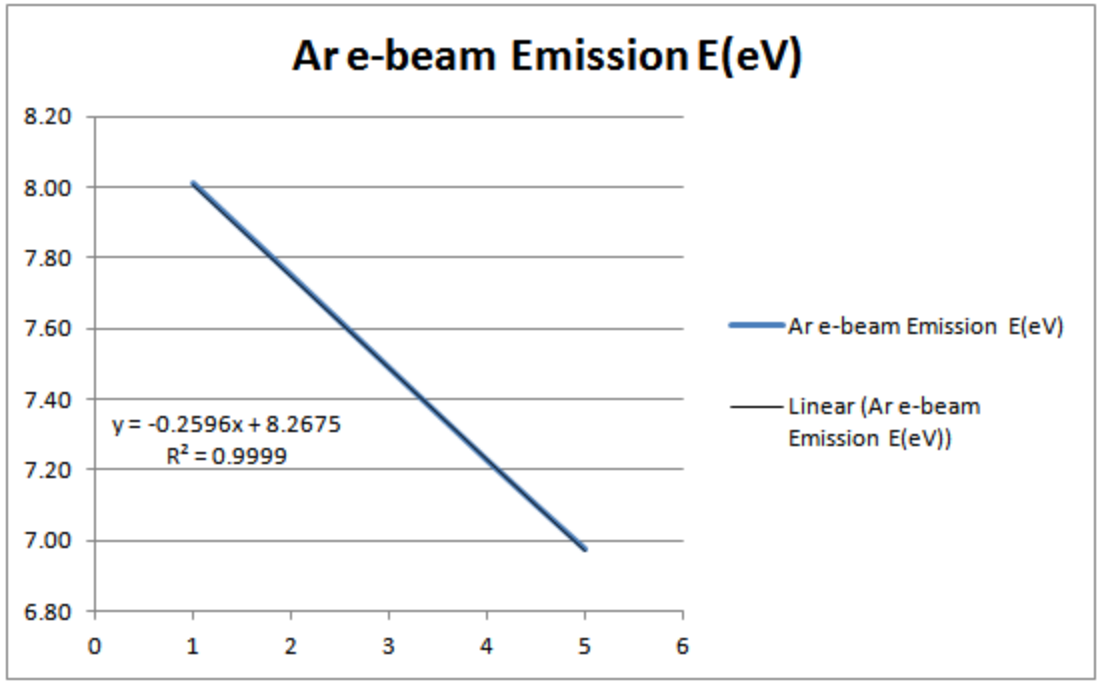

From Ar spectra N104403/2004		
J	e-beam lambda (nm)	Ar e-beam Emission E(eV)
1	154.8	8.01
2	160.0	7.75
3	165.6	7.49
4	171.6	7.23
5	177.8	6.97
	Slope =	-0.2596
	Intercept=	8.2675

E-beam Emission
Hydrino $H_2(1/4)$ Ro-vibrational P Branch

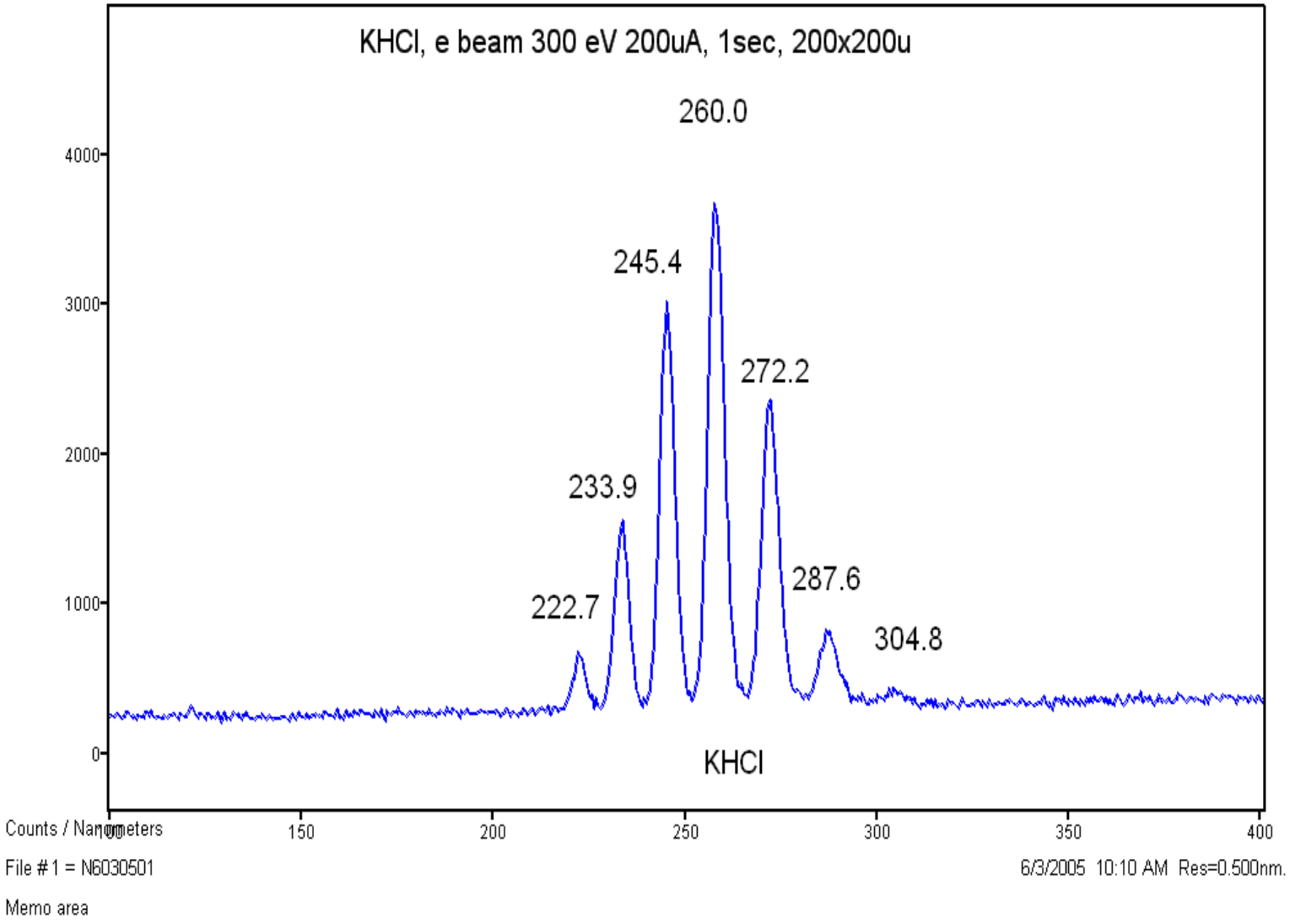

E-beam Emission
Hydrino $H_2(1/4)$ Ro-vibrational P Branch is Dependent on Temperature which is Confirmation of Ro-Vibrational Assignment

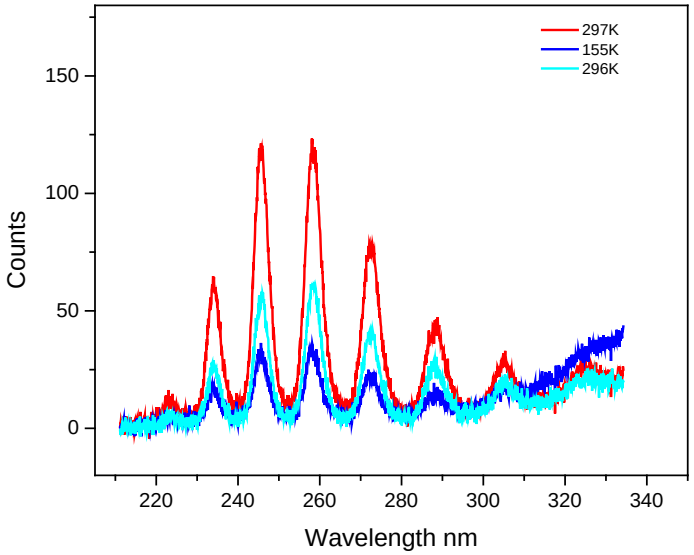

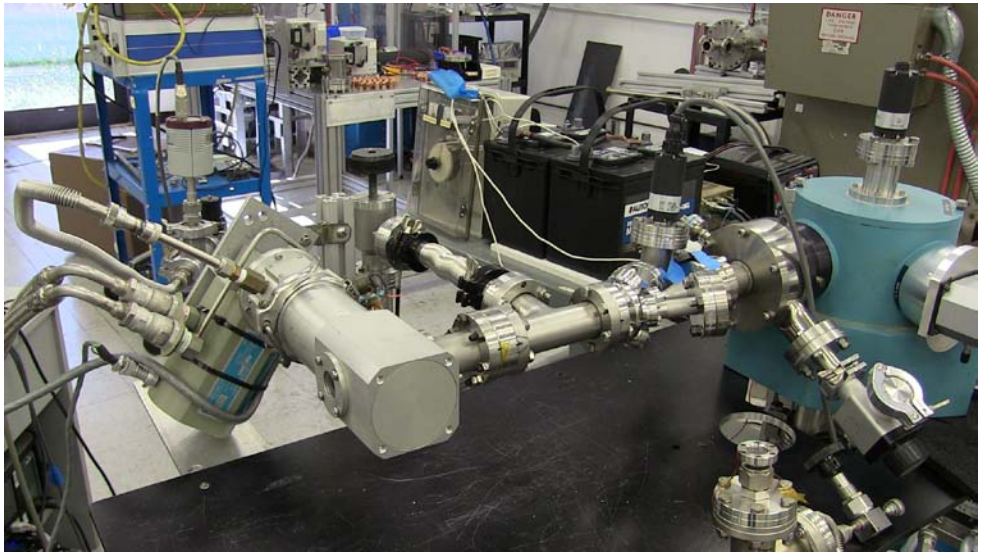

E-beam Emission Linear Regression

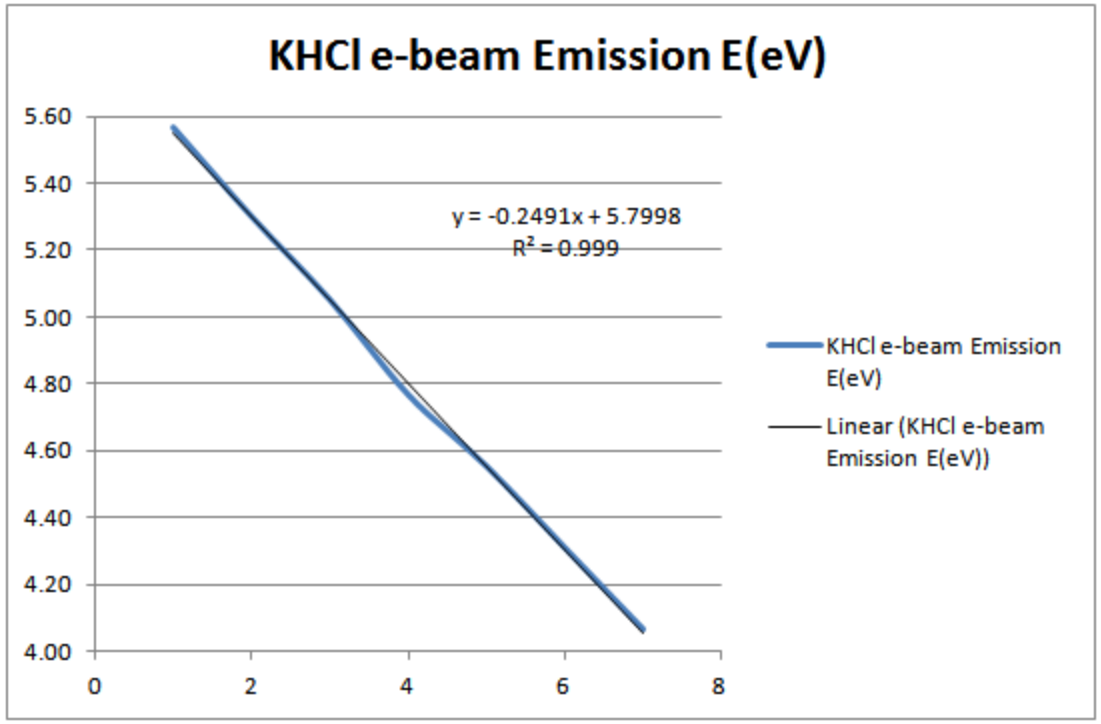

From KHCl spectra N6030501 6/3/2005		
J	e-beam lambda (nm)	KHCl e-beam Emission E(eV)
1	222.7	5.57
2	233.9	5.30
3	245.4	5.05
4	260.0	4.77
5	272.2	4.55
6	287.6	4.31
7	304.8	4.07
	Slope =	-0.2491
	Intercept=	5.7998

Vibrational and Rotational Predicted Energies

• Hydrogen molecular vibrational energy, E_{vib}, for the v = 0 to v = 1 transition of hydrogen type molecules $H_2(1/p)$ is given as (Eq. 11.223 of Ref [1]):

$$E_{vib} = p^2 \times 0.515912\ eV$$

• The rotational energies, E_{rot}, for the J to J+1 transition of hydrogen molecules $H_2(1/p)$ is given as (Eq. 12.74 of Ref [1]):

$$E_{rot} = p^2 \times (J+1) \times 0.01509\ eV$$

• For example, for hydrogen and the first five hydrino states, this yields predicted vibrational (v=0 to 1) and rotational (J=0 to 1) energies of:

p	State (H2(1/p))	Vibrational Energy (eV)	Rotational Energy (eV)
1	H2	0.5159	0.01509
2	H2(1/2)	2.0636	0.06036
3	H2(1/3)	4.6431	0.13581
4	H2(1/4)	8.2544	0.24144
5	H2(1/5)	12.8976	0.37725
6	H2(1/6)	18.5725	0.54324

Gas and Impregnated Crystal E-beam Emission Assignment

• The emitters in both HOH-Ar and a solid impregnated with hydrino gas match emission spacing's and match the rotationally predicted energies for $H_2(1/4)$. The emitter in HOH-Ar matches the vibrationally predicted energy for $H_2(1/4)$.

H2(1/4) in Ar	Experimental Value (eV)	Theoretical Value (eV)
Vibrational Energy (v = 0 to 1)	8.2675	8.2544
Rotational Energy (J = 0 to 1)	0.2596	0.2414

H2(1/4) in KHCl	Experimental Value (eV)	Theoretical Value (eV)
Vibrational Energy (v = 0 to 1)	5.7998	*
Rotational Energy (J = 0 to 1)	0.2491	0.2414

• *The vibrational energy for $H_2(1/4)$ in a solid matrix is shifted due to the increased effective mass from the solid matrix interaction analogous to the cases of H_2 in solid matrices such as Si and Ge as discussed in primary literature.

[1]: R. Mills, The Grand Unified Theory of Classical Physics; September 2016 Edition, posted at http://brilliantlightpower.com/book-download-and-streaming/

Raman Confirmation of Molecular Hydrino of $H_2(1/4)$ Ro-Vibrational Band

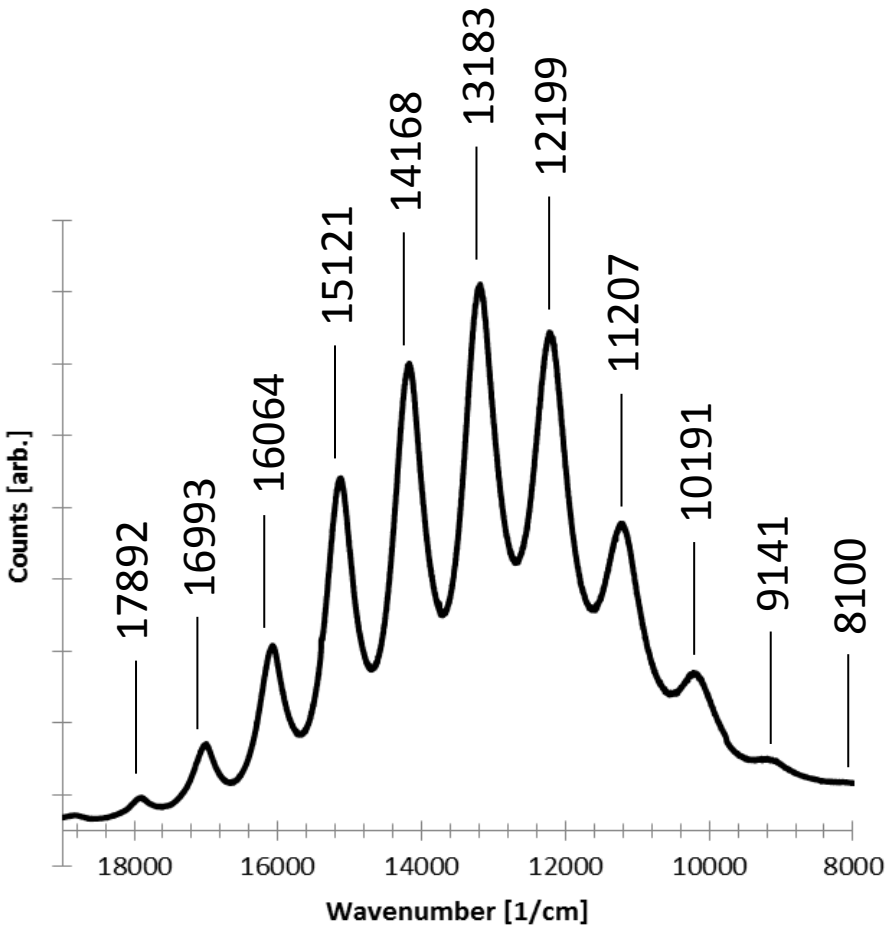

Raman-mode second-order photoluminescence spectrum of the KOH-KCl (1:1 wt.) getter exposed to a solid fuel initiation of samples of 70mg Cu with 30mg deionized water contained in a 75mg Al crucible in an Ar atmosphere using a Horiba Jobin Yvon LabRam ARAMIS 325nm laser.

Comparison of the Transition Energies and Transition Assignments with the Observed Raman Peaks

Assignment	Calculated (cm^{-1})	Experimental (cm^{-1})	Difference (%)
P(5)	18,055	17,892	0.91
P(4)	17,081	16,993	0.52
P(3)	16,107	16,064	0.27
P(2)	15,134	15,121	0.08
P(1)	14,160	14,168	-0.06
Q(0)	13,186	13,183	0.02
R(0)	12,212	12,199	0.11
R(1)	11,239	11,207	0.28
R(2)	10,265	10,191	0.73
R(3)	9,291	9,141	1.65
R(4)	8,318	8,100	2.69

Plot Comparison Between the Theoretical Energies and Observed Raman Spectral Assignments

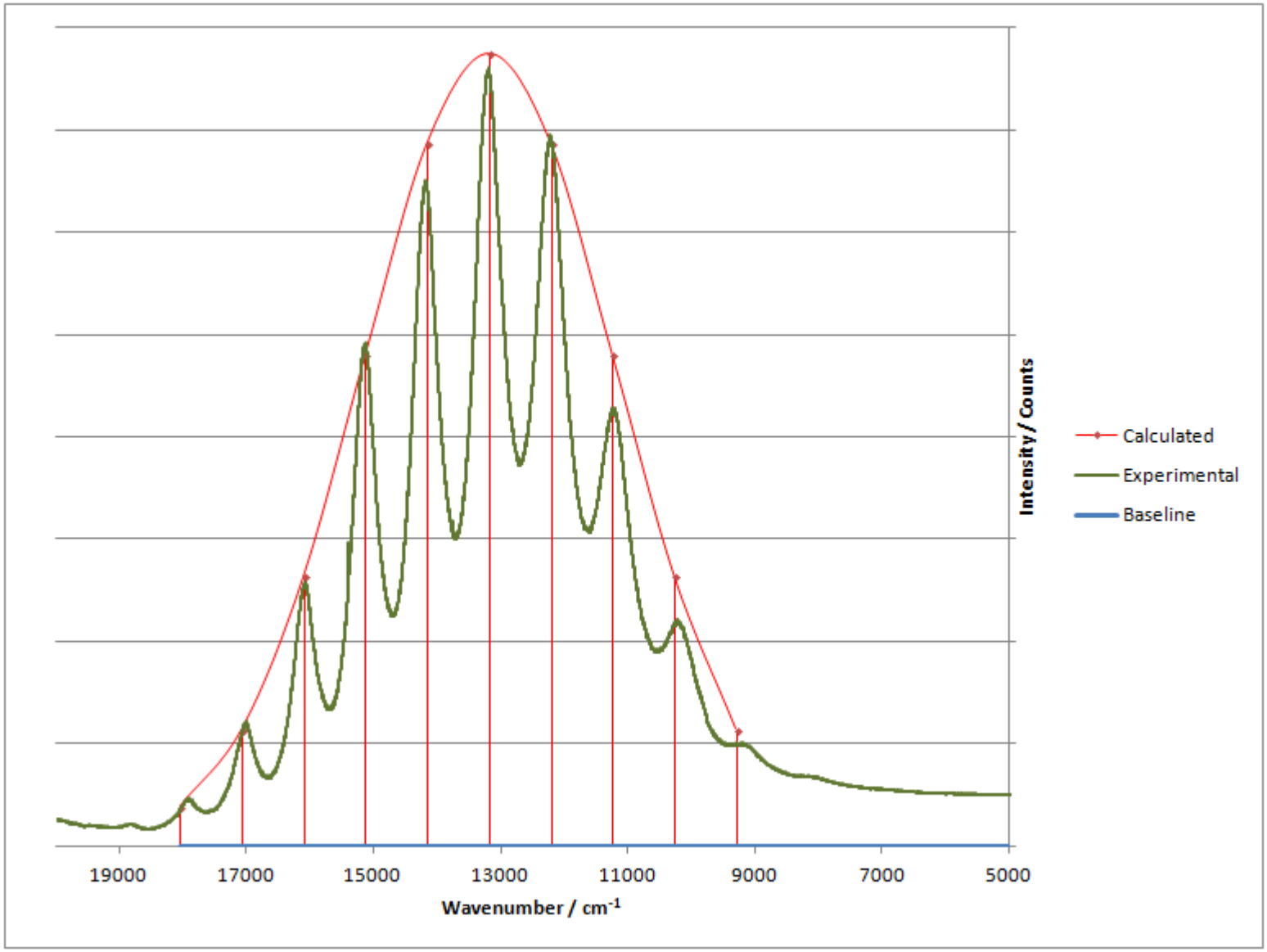

Raman Confirmation of Molecular Hydrino of $H_2(1/4)$ Rotational Energy

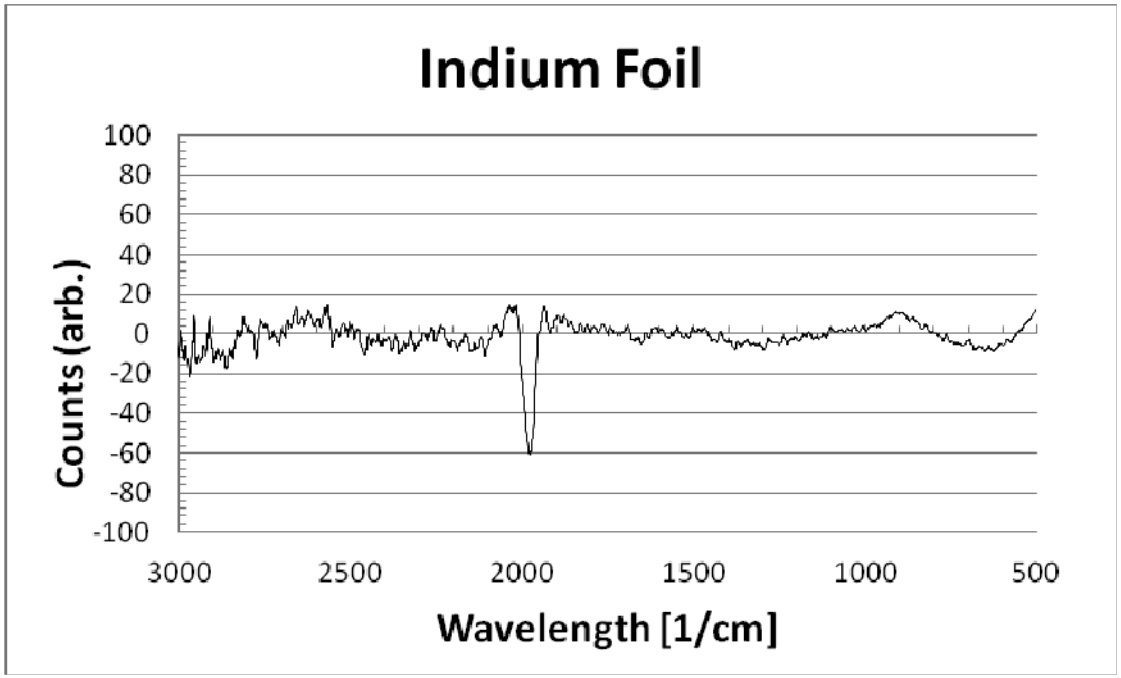

The Raman spectrum obtained on a In metal foil exposed to the product gas from a series of solid fuel ignitions under argon, each comprising 100 mg of Cu mixed with 30 mg of deionized water. Using the Thermo Scientific DXR SmartRaman spectrometer and the 780 nm laser, the spectrum showed an inverse Raman effect peak at 1982 cm^{-1} that matches the free rotor energy of $H_2(1/4)$ (0.2414 eV).

Raman Confirmation of Molecular Hydrino of $H_2(1/4)$ Rotational Energy

Raman spectra obtained using the Thermo Scientific DXR SmartRaman spectrometer and the 780 nm laser on copper electrodes pre and post ignition of a 80 mg silver shot comprising 1 mole% H_2O, wherein the detonation was achieved by applying a 12 V 35,000 A current with a spot welder. The spectra showed an inverse Raman effect peak at about 1940 cm^{-1} that matches the free rotor energy of $H_2(1/4)$ (0.2414 eV).

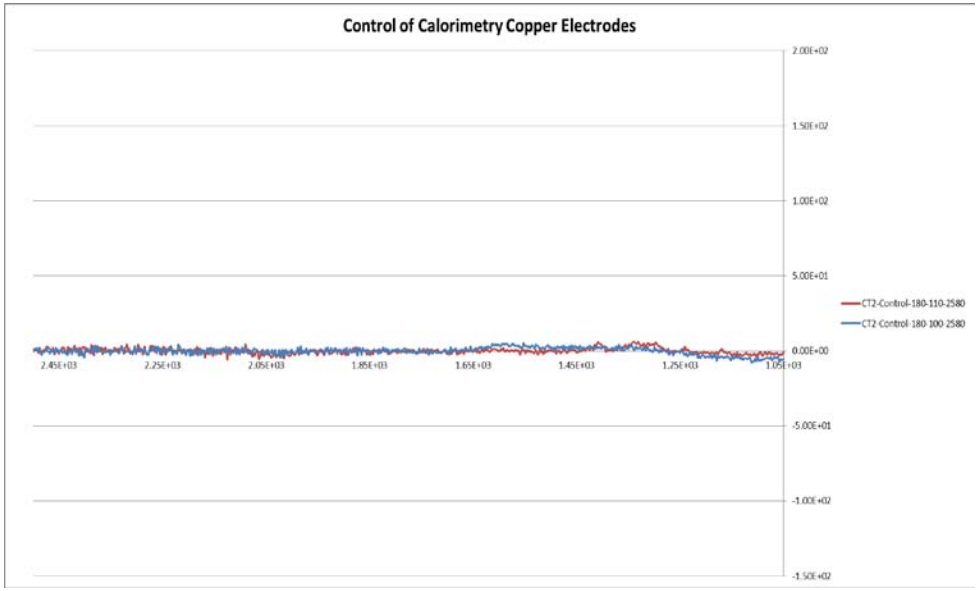

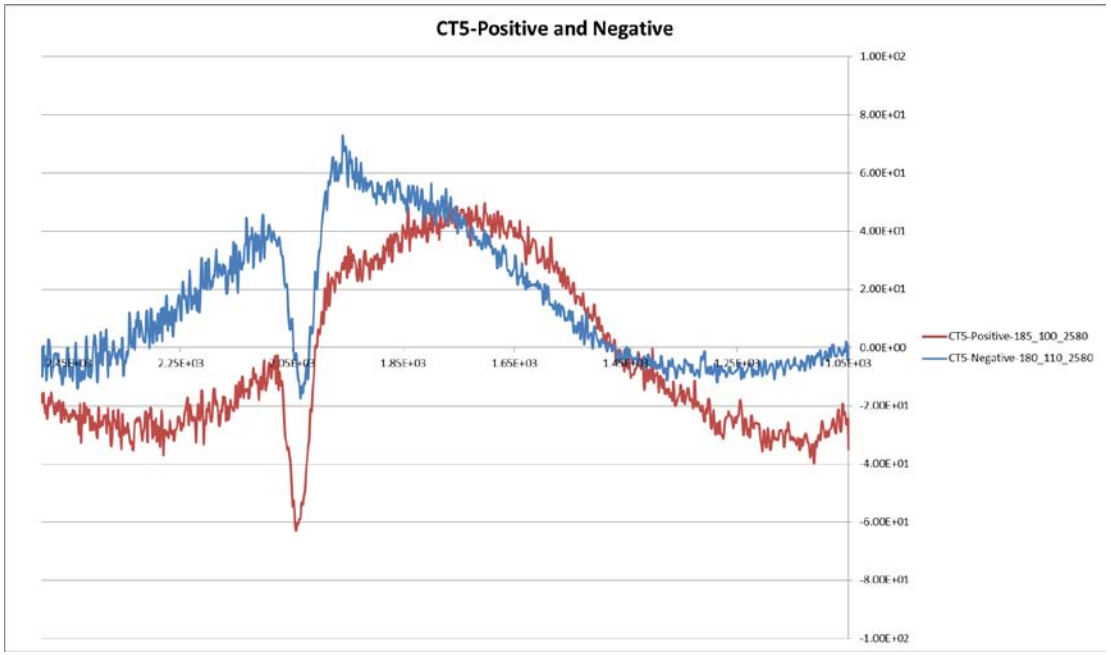

Raman Confirmation of Molecular Hydrino of $H_2(1/4)$ Rotational Energy of Hydrino Web Compound

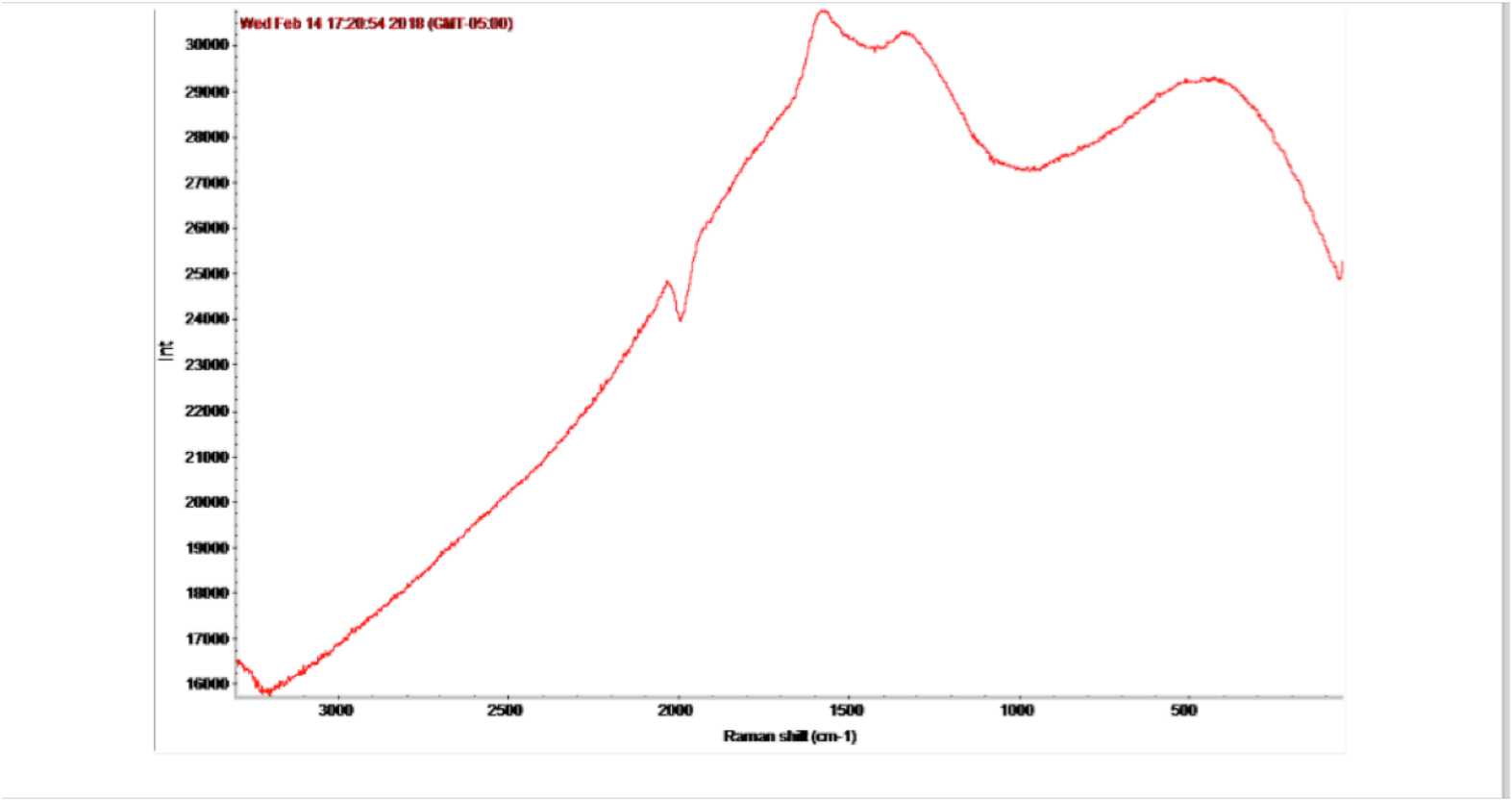

E-beam Emission
Hydrino $H_2(1/4)$ Ro-vibrational P Branch of Web Compound Matches that of Gaseous $H_2(1/4)$ Spectrum

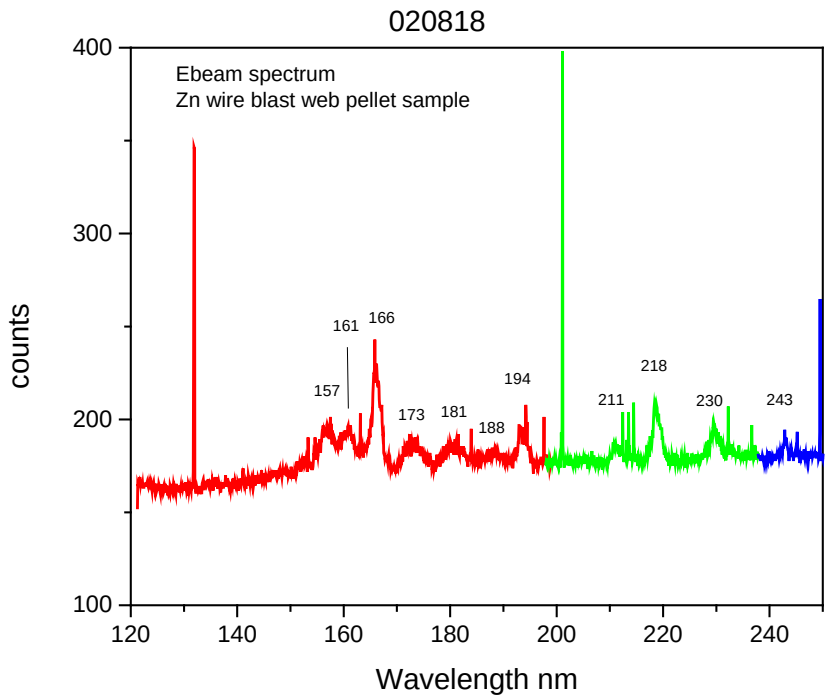

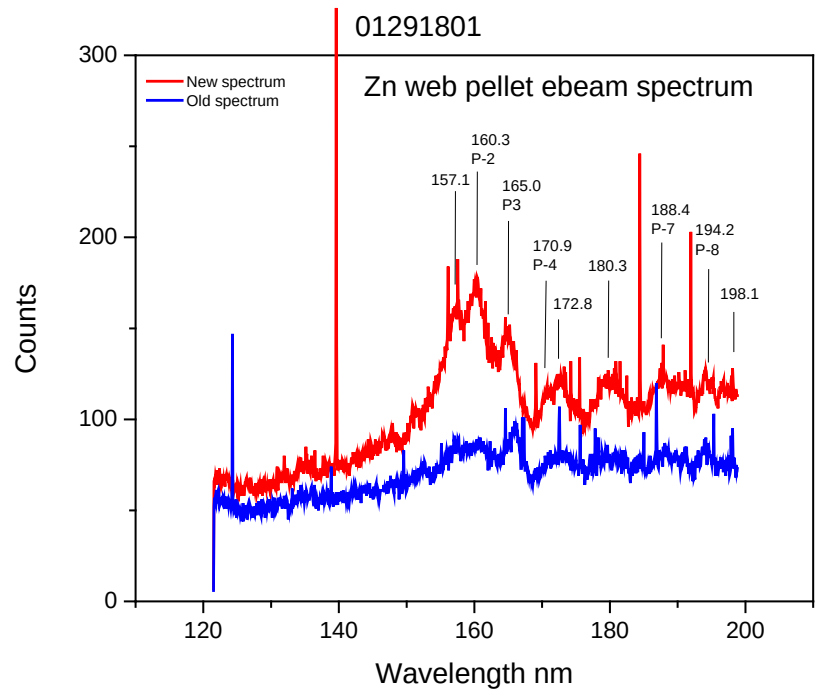

E-beam Emission
Hydrino $H_2(1/4)$ Ro-vibrational P Branch of Web Compound Matches that of Gaseous $H_2(1/4)$ Spectrum

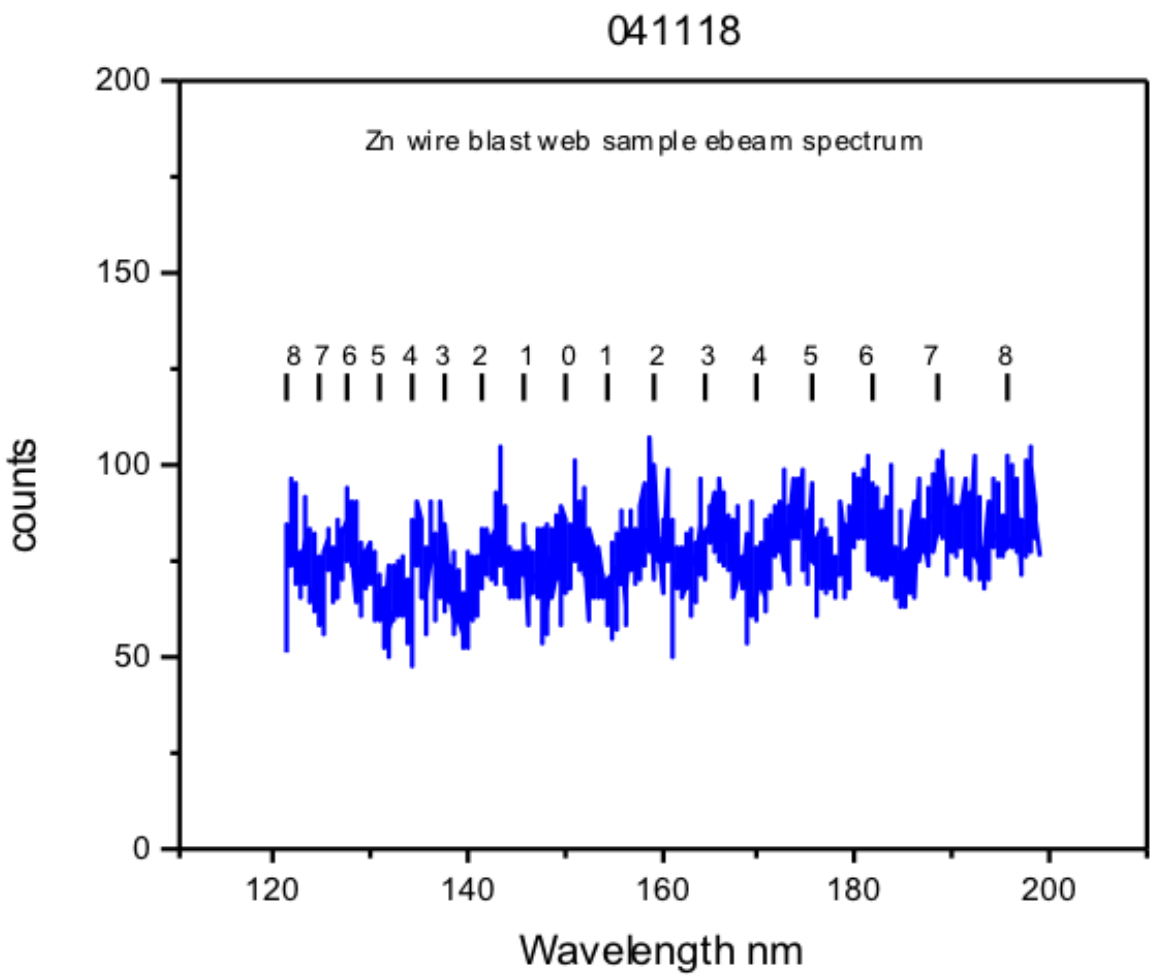

XPS Total Binding Energy of $H_2(1/4)$

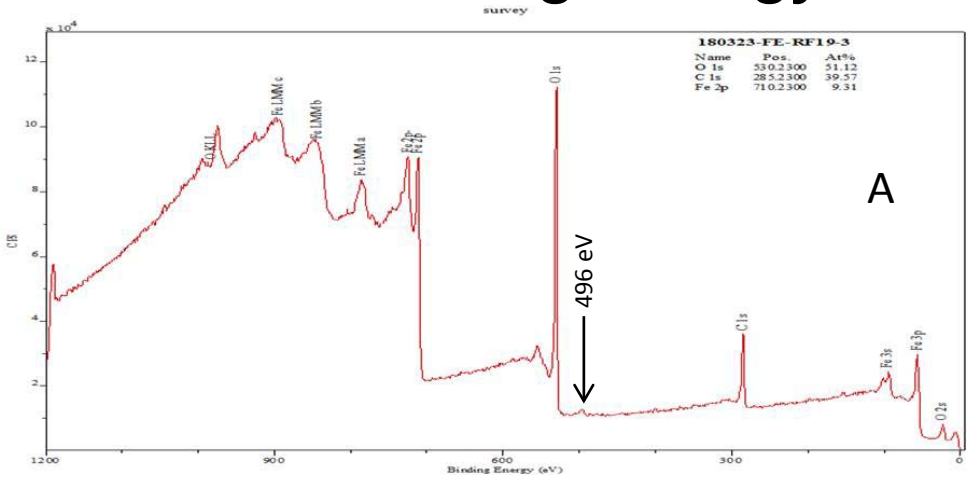

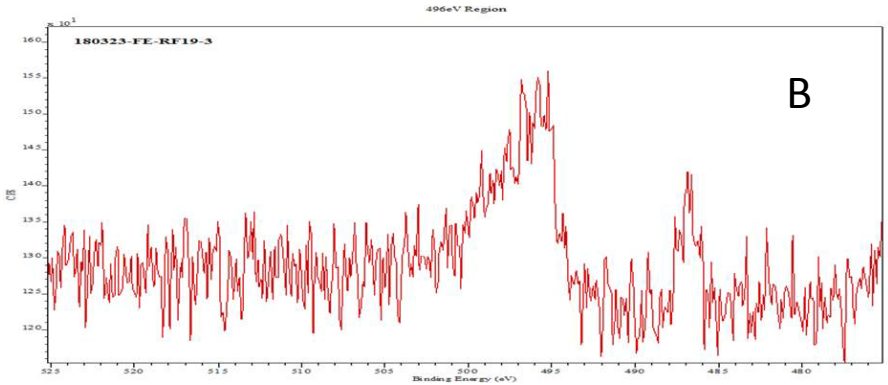

The XPS spectra of the hydrino Fe web compound having a peak at 496 eV assigned to $H_2(1/4)$ wherein other possibilities such Na, Sn, and Zn were eliminated since only Fe, O, and C peaks are present and other peaks of the candidates are absent. A. Survey scan. B. High resolution scan in the region of the 496 eV peak of $H_2(1/4)$.

XPS Total Binding Energy of $H_2(1/4)$

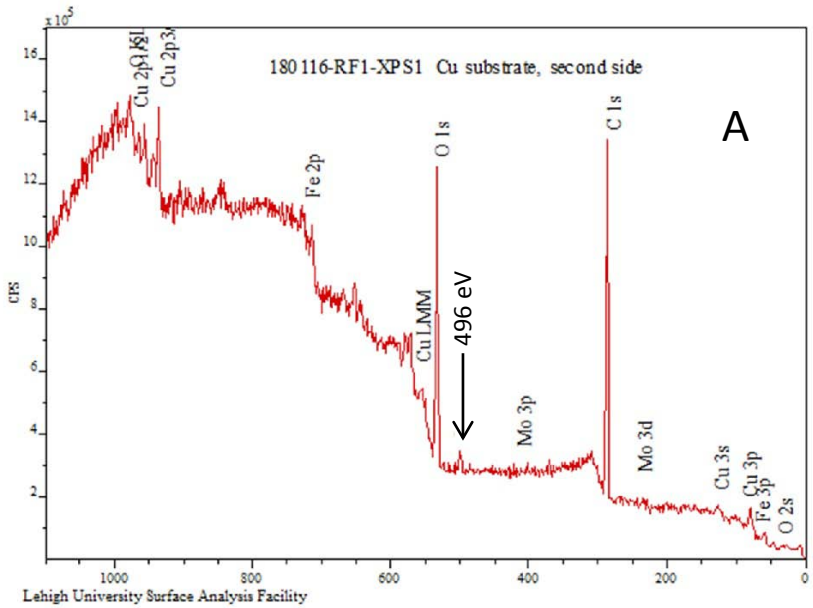

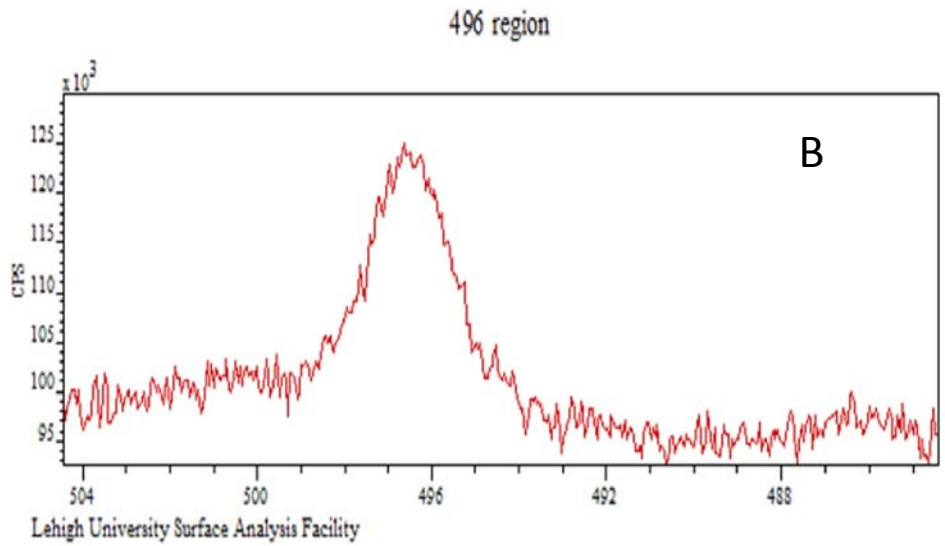

The XPS spectra of the hydrino Mo web compound having a peak at 496 eV assigned to $H_2(1/4)$ wherein other possibilities such Na, Sn, and Zn were eliminated since only Mo, O, and C peaks are present and other peaks of the candidates are absent. Mo 3s which is less intense than Mo3p was at 506 eV with additional samples that also showed the $H_2(1/4)$ 496 eV peak. A. Survey scan. B. High resolution scan in the region of the 496 eV peak of $H_2(1/4)$.

XPS Confirmation of Molecular Hydrino of $H_2(1/4)$ Binding Energy

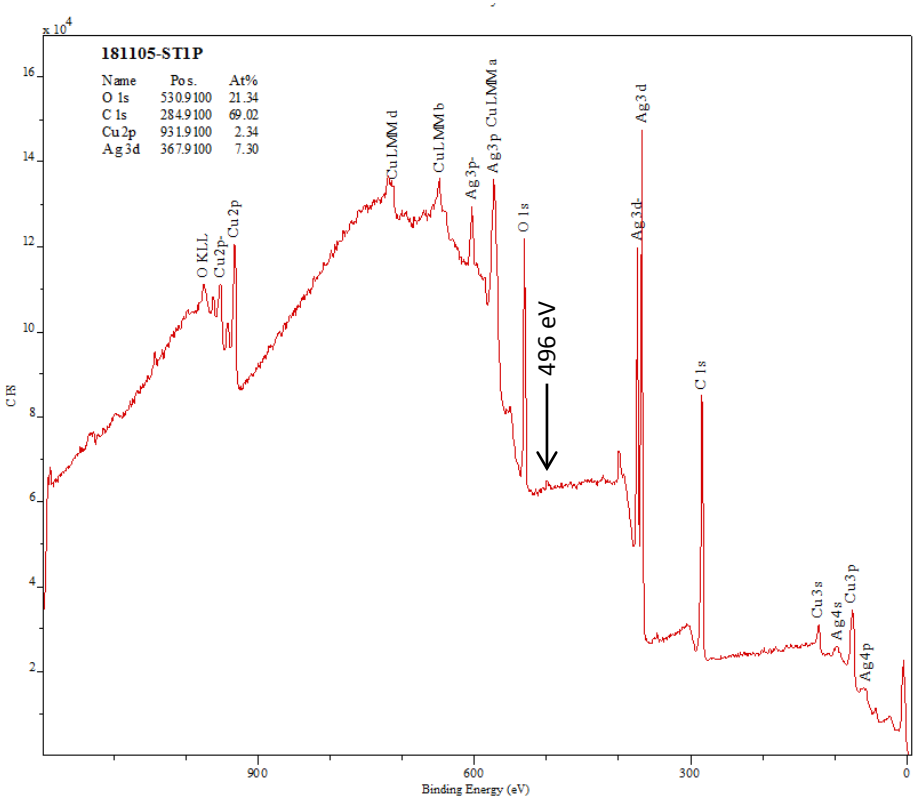

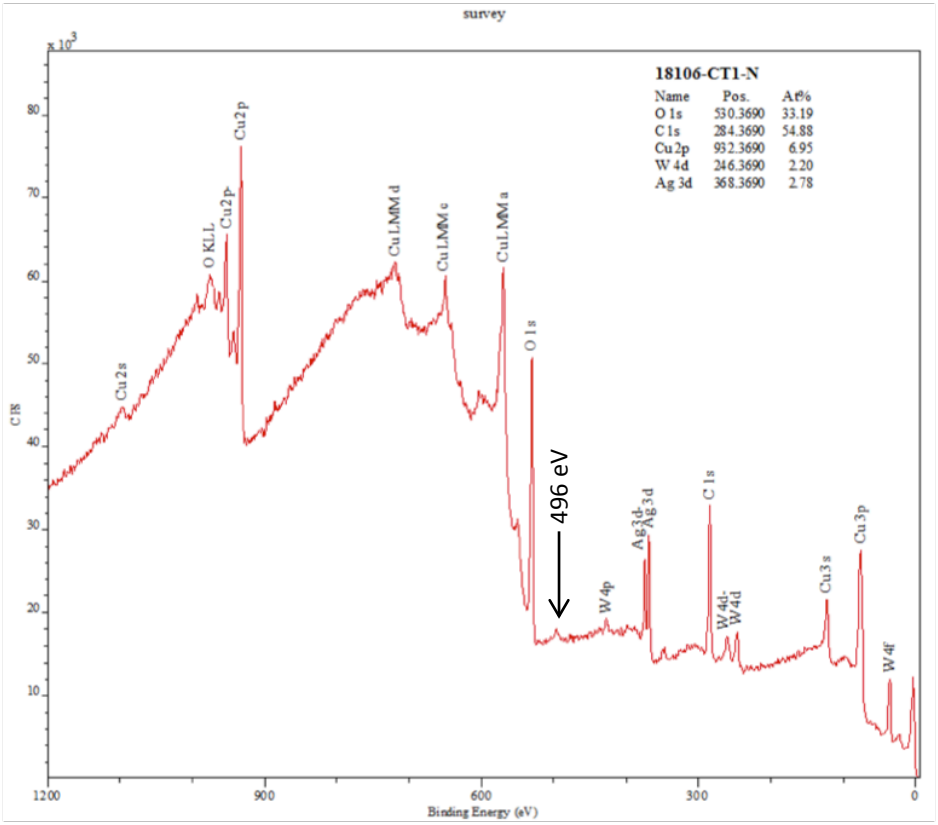

The XPS spectra on copper electrodes post ignition of a 80 mg silver shot comprising 1 mole% H_2O, wherein the detonation was achieved by applying a 12 V 35,000 A current with a spot welder. The peak at 496 eV was assigned to $H_2(1/4)$ wherein other possibilities such Na, Sn, and Zn were eliminated since the corresponding peaks of these candidates are absent. Raman post detonation spectra showed an inverse Raman effect peak at about 1940 cm^{-1} that matches the free rotor energy of $H_2(1/4)$ (0.2414 eV).

Extraordinary EPR Spectrum of Hydrino Web Compound And Solid Fuel Reaction Product

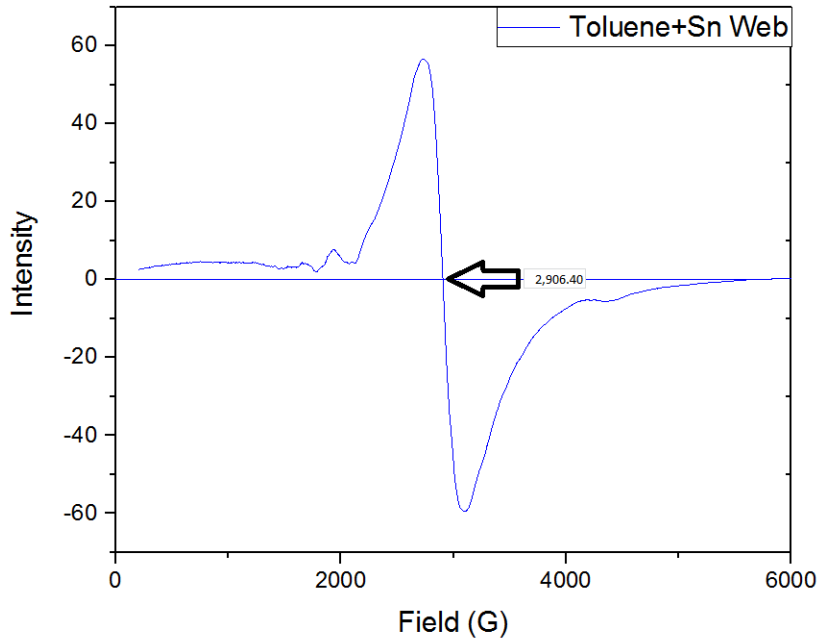

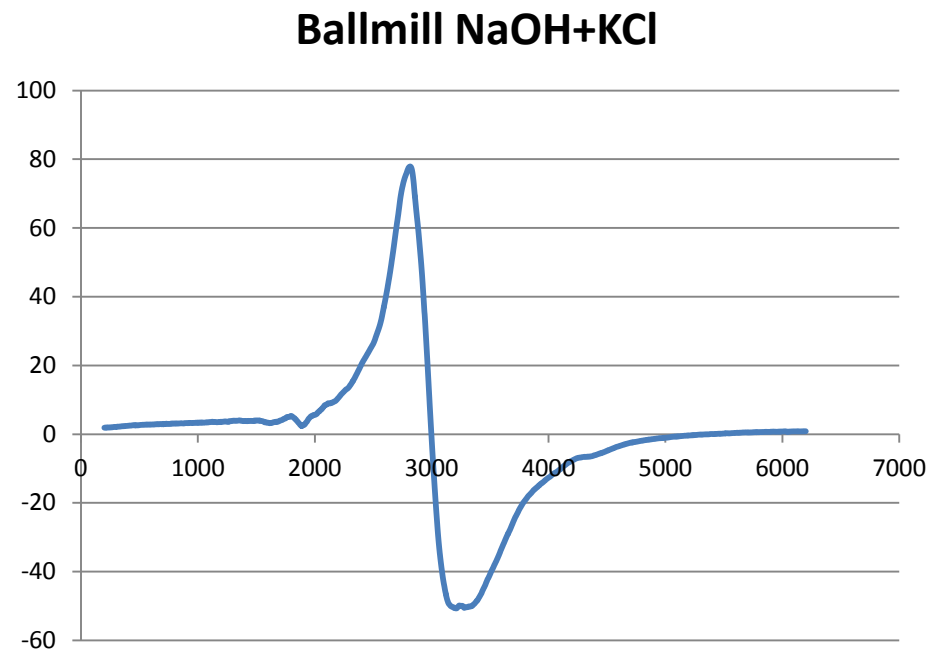

- No known EPR active species present.
- Shift of 474 G matches theoretical, ΔH = 375 G.
- The main parameters of EPR spectrum of tin hydroxyl and superoxide radicals: g-factor and line width ΔH, calculated from the EPR spectra are following: g1 =2.0021 and ΔH1 =1 G, g2 =2.0009 and ΔH2 =0.8 G.

Effect of Cryogenic Temperature on EPR Spectrum of Zinc Hydrino Compound

The molecular hydrino dimer EPR peak shift of about 474 G was observed at 298K (red trace) and was absent at 77K (blue trace) which is evidence of the predicted hydrino phase change to a compact solid at cryogenic temperatures wherein the magnetism due to dense packing causes the EPR peak to be broadened and out of range.

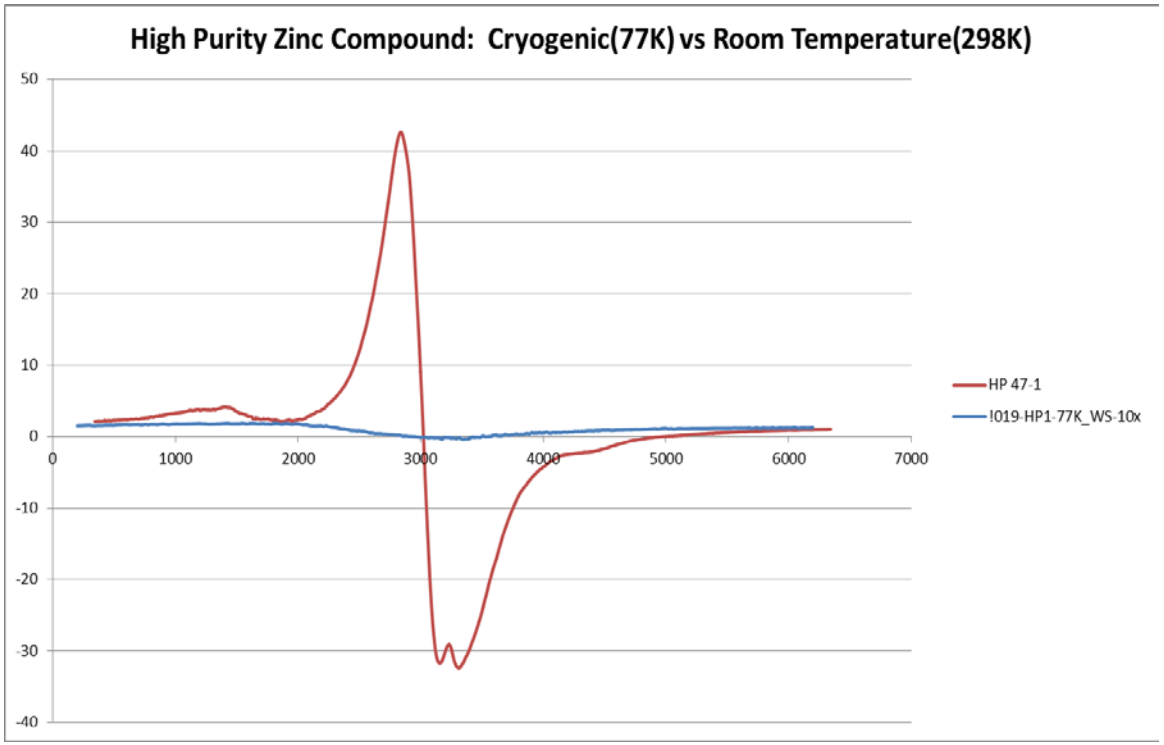

MoWeb: Vibrating Sample Magnetometer

- Paramagnetic material responds linearly with the induced magnetism.
- The observed “S” shape is characteristic of super paramagnetic, a hybrid of ferromagnetism and para magnetism.
- It is exception that the induced magnetism peaks at 5K Oe and declines with higher applied field.

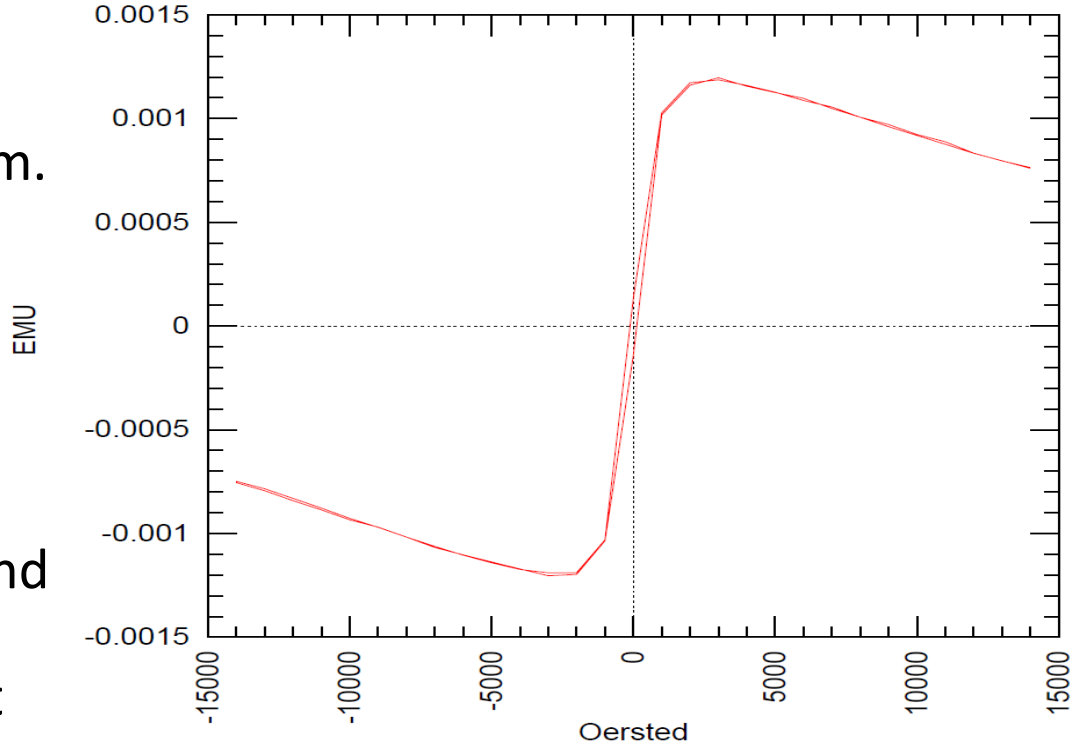

FTIR of Tungsten Hydrino Web Compound that Shows Only the Hydrino Molecular Dimer $[H_2(1/4)]_2$ Vibrational Band at 720 cm^{-1}

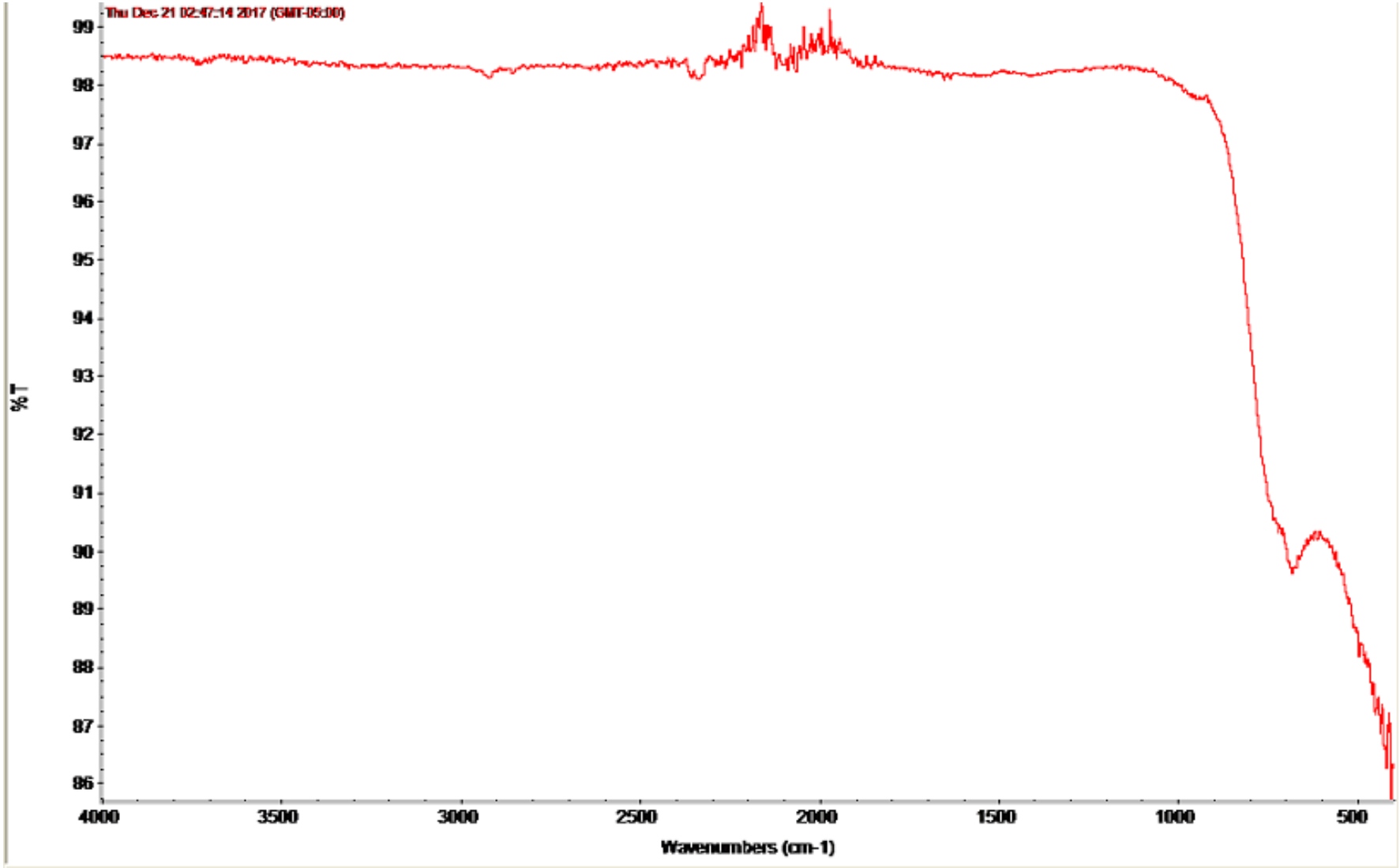

ToF-SIMS Spectrum of K_2CO_3-KCl (30:70 wt%) getter exposed to hydrino gas and having upfield shifted MAS NMR spectral peaks.

Multimer clusters of matrix compounds with di-hydrogen as part of the structure, $M:H_2$ (M = KOH or K_2CO_3) such as and consistent with $H_2(1/p)$ as a complex in the structure were observed. These clusters were not observed in controls comprising the matrix exposed to H_2.

Positive ToF-SIMS, m/e = 90 to 100 region

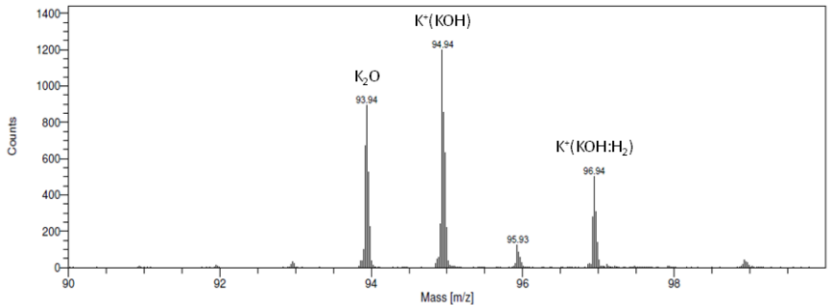

Positive ToF-SIMS, m/e = 0 to 200 region.

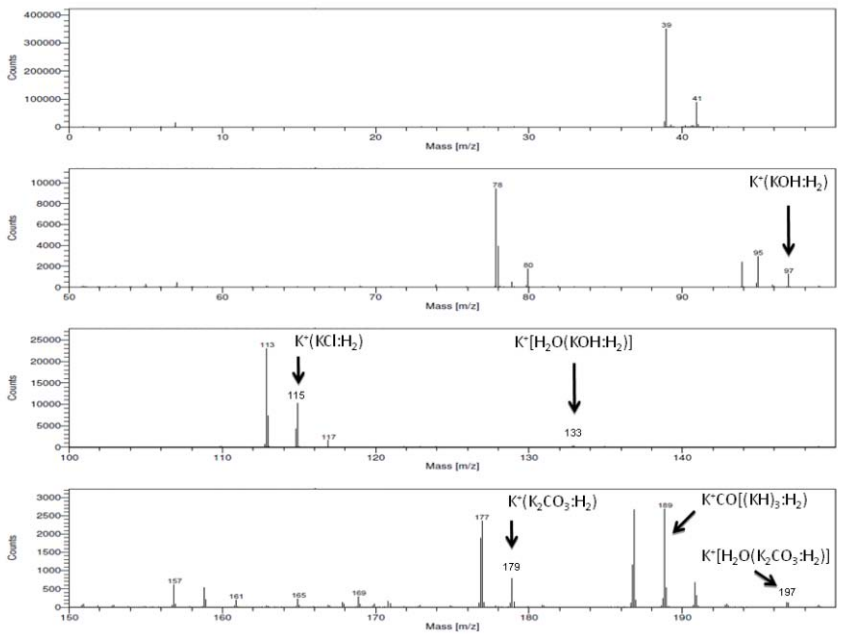

ToF-SIMS Spectrum of K_2CO_3-KCl (30:70 wt%) getter exposed to hydrino gas and having upfield shifted MAS NMR spectral peaks cont'd.

Positive ToF-SIMS, m/e = 200 to 1000 region.

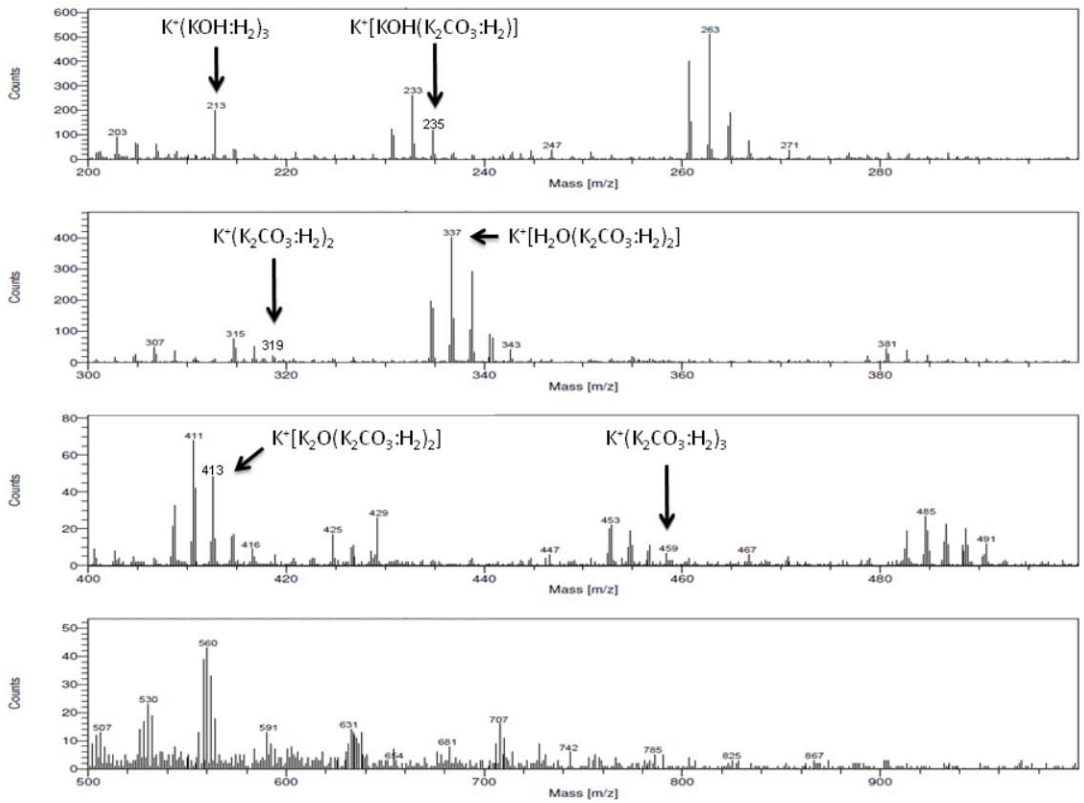

Gas Chromatography with Hydrogen Carrier Gas Showing Hydrino Peak at 73 Minutes as Negative Eliminating Any Other Assignment

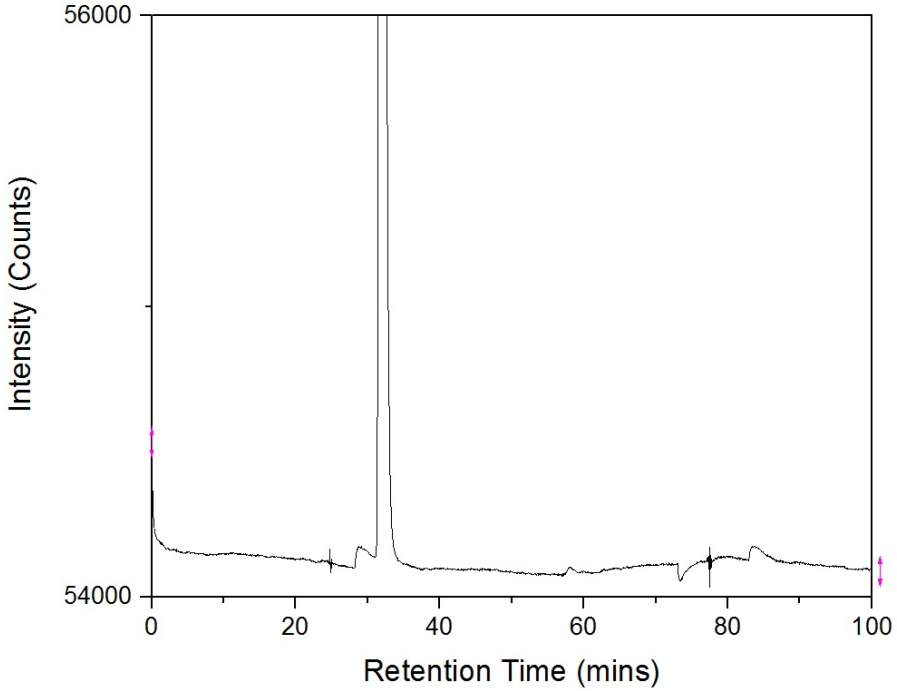

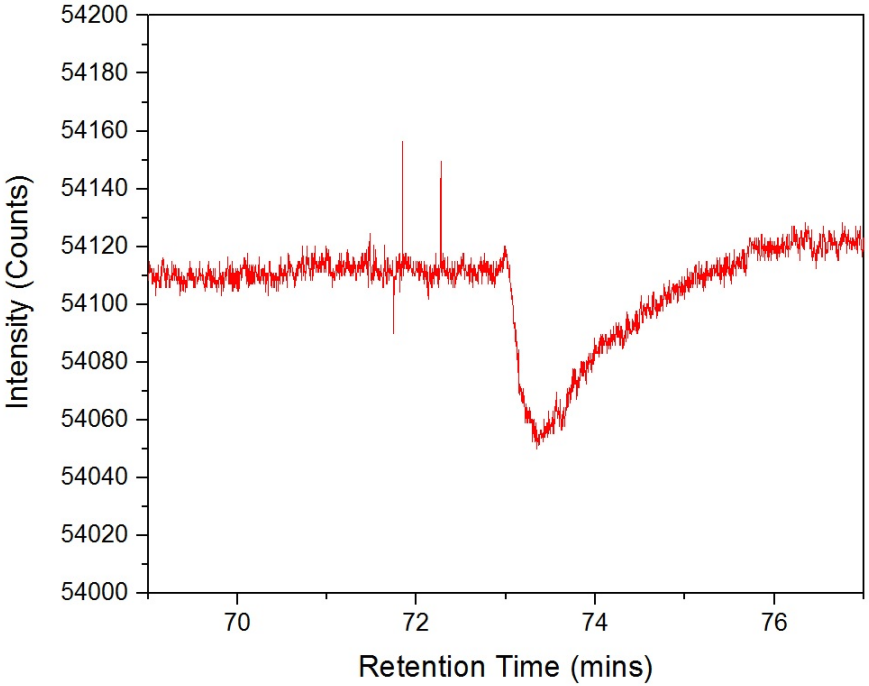

^{1}H MAS NMR Spectra

^{1}H MAS NMR spectrum relative to external TMS of the initial KOH-KCl (1:1) getter that shows the known down-field shifted matrix peak at +4.41 ppm.

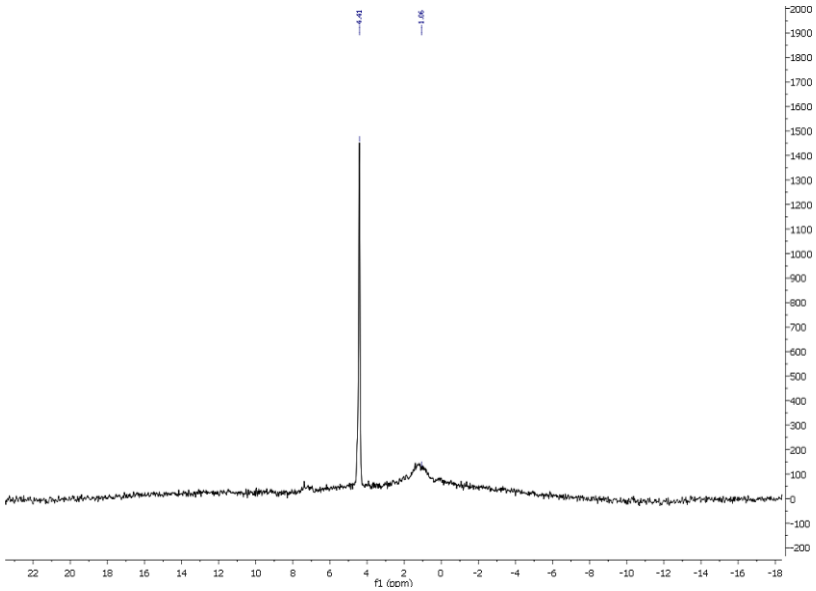

^{1}H MAS NMR spectrum relative to external TMS of the KOH-KCl (1:1) getter exposed to hydrino gas that shows upfield shifted matrix peaks at -4.06 and -4.41 ppm due to the magnetism of molecular hydrino.

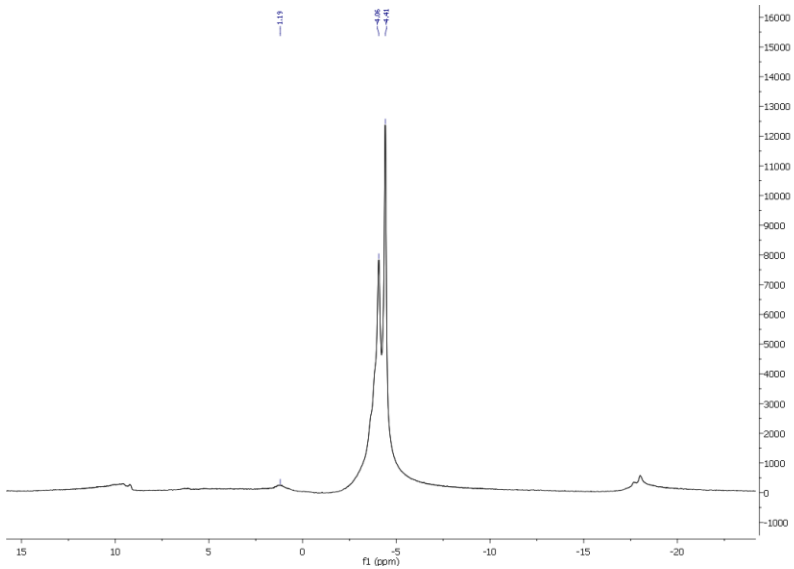

4.6 MW Characteristic H to $H_2(1/4)$ Transition EUV Continuum Radiation with a Predicted 10.1 nm Cutoff

- Hydrated silver shots comprising a source of H and HOH catalyst were ignited by passing a low voltage, high current through the shot to produce explosive plasma that emitted brilliant light predominantly in the short-wavelength 10 to 300 nm region.

- The peak power of 20 MW and time-average power of 4.6 MW was measured using absolute spectroscopy over the 22.8-647 nm region wherein the optical emission energy was 250 times the applied energy.

- The wavelength calibrated and absolute intensity calibrated spectrum (10-45 nm) of the emission of hydrated silver shots recorded on the GIS with a Zr filter showed the EUV continuum cutoff at 10.1 nm.

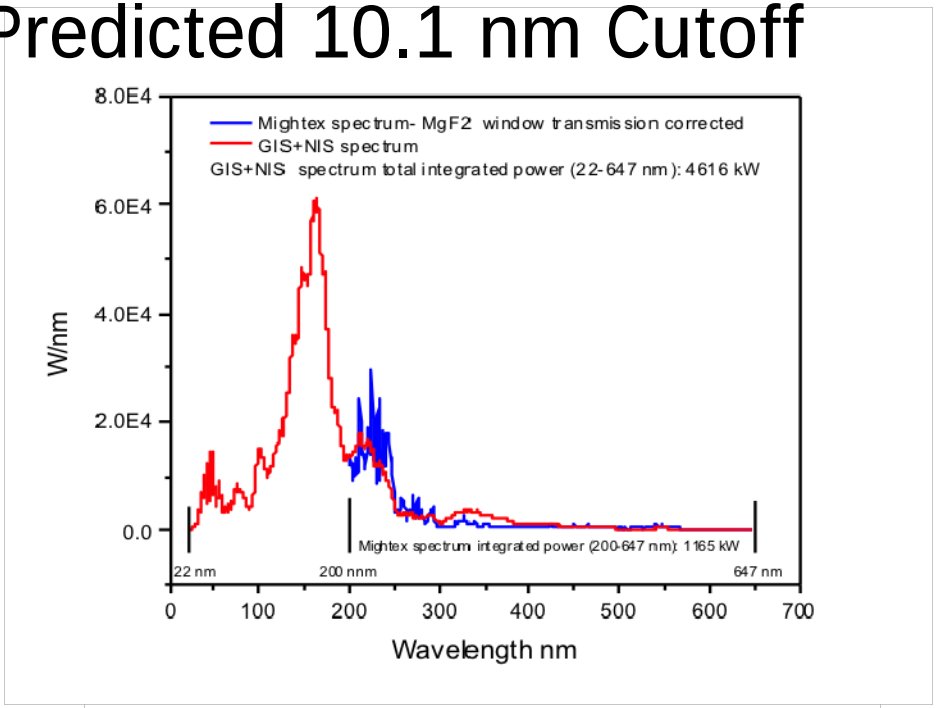

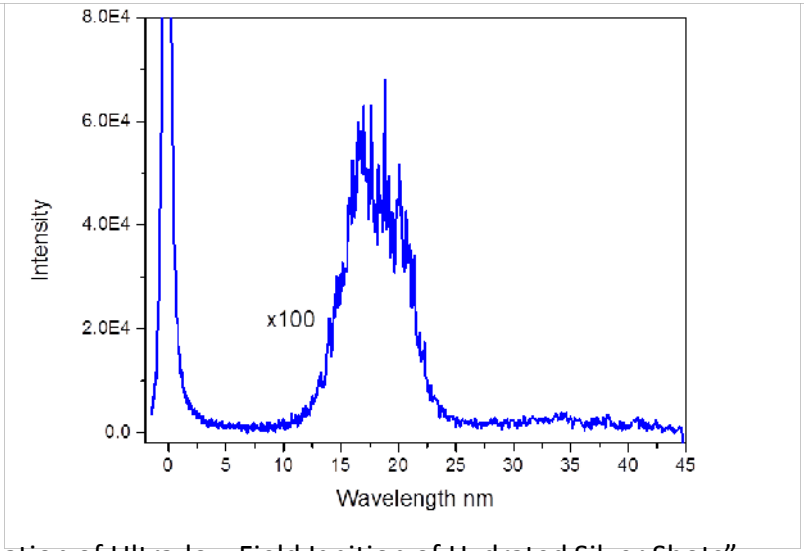

R. Mills, Y. Lu, R. Frazer, "Power Determination and Hydrino Product Characterization of Ultra-low Field Ignition of Hydrated Silver Shots", Chinese Journal of Physics, Vol. 56, (2018), pp. 1667-1717.

Massive Ionization Determined by Stark Broadening

- Stark broadening of the H alpha line of 1~1.3 nm corresponds to an electron density of 2.4-3.5X10^{23}/m^3.
- The SunCell® gas density was calculated to be 2.5X10^{25} atoms/m^3 based on an argon-H_2 pressure of 800 Torr and temperature of 3000K.
- The corresponding ionization fraction was about 10%.
- Given that argon and H_2 have ionization energies of about 15.5 eV and a recombination lifetime of less than 100 us at high pressure, the power density to sustain the ionization is

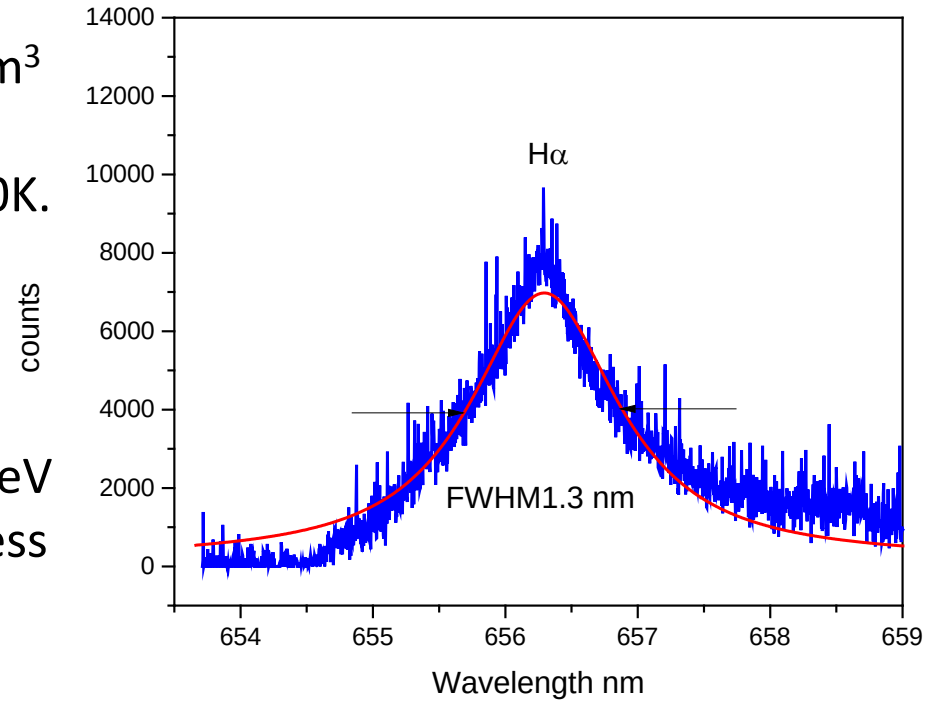

$$P = \left(\frac{3.5X10^{23}\,electrons}{m^3}\right)\left(15.5\ eV\right)\left(\frac{1.6X10^{-19}\,J}{eV}\right)\left(\frac{1}{10^{-4}\,s}\right) = \frac{8.7X10^{9}\,W}{m^3}$$

Thank you!

For more information please visit us at www.brilliantlightpower.com